Title

DIFFUSION CONTROLLED MULTI-SWEEP CYCLIC VOLTAMMETRY I. REVERSIBLE DEPOSITION ON A ROTATING DISC ELECTRODE

Author

Ross, F.N.

Publication Date

1982-06-01

LBL-14524
Preprint

Lawrence Berkeley Laboratory
UNIVERSITY OF CALIFORNIA

Materials & Molecular
Research Division

To be published in the Journal of the Electrochemical Society

DIFFUSION CONTROLLED MULTI-SWEEP CYCLIC VOLTAMMETRY I. REVERSIBLE DEPOSITION ON A ROTATING DISC ELECTRODE

P.C. Andricacos and P.N. Ross, Jr.

June 1982

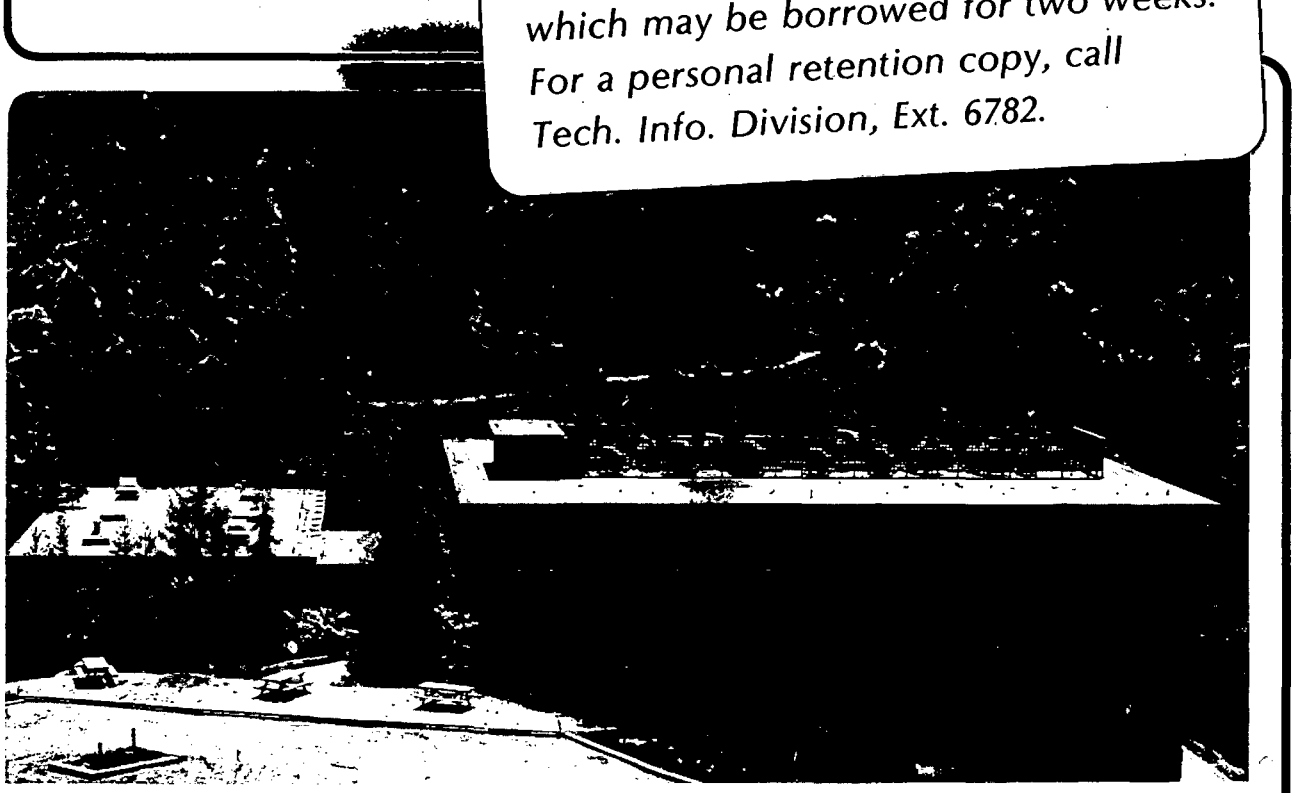

Prepared for the U.S. Department of Energy under Contract DE-AC03-76SF00098

DISCLAIMER

DIFFUSION CONTROLLED MULTI-SWEEP CYCLIC VOLTAMMETRY

I. REVERSIBLE DEPOSITION ON A ROTATING DISC ELECTRODE

P. C. Andricacos and P. N. Ross, Jr.
Materials and Molecular Research Division
Lawrence Berkeley Laboratory
University of California
Berkeley, CA 94720

ABSTRACT

A model is proposed for the behavior of a diffusion controlled reversible deposition reaction occurring on a rotating disc electrode under conditions of multi-sweep cyclic voltammetry. Results are presented for dimensionless concentration, current density, and charge density functions, obtained by the application of the Nernst-Siver approximation for transient convective diffusion. The existence of a periodic state is demonstrated for cycle times of the order of the characteristic time for the rotating disc. Diagnostic criteria of potential electroanalytical use associated with the periodic state are developed in terms of dimensionless sweep rate, reversal time, and cathodic reversal overpotential. It is found that significant differences exist in the current and concentration functions as determined during the first and second - also periodic - cathodic sweeps. The potentiodynamic determination of diffusion limiting current densities as well as the applicability of a triangular periodic potential waveform in plating are also briefly discussed.

Key Words: Electrode, deposition, mass transport, voltammetry.

This work was supported by the Assistant Secretary for Conservation and Renewable Energy, Office of Advanced Conservation Technology, Division of Electrochemical Systems Research of the U.S. Department of Energy under Contract DE-AC03-76SF00098.

Introduction

It has been demonstrated (1,2) that the application of periodic current pulses to a rotating disk electrode (RDE) gives rise to an output signal which also becomes periodic after a short time. In multi-sweep cyclic voltammetry (CV), a periodic triangular potential waveform is applied to the electrode and one might therefore expect the current response to become periodic after the passage of relatively few cycles. The purpose of the present investigation is to define conditions for the rapid attainment of the periodic state and to describe the characteristics of the periodic state when electrodeposition reactions are studied by multi-sweep CV.

In the analyses to be presented, we examine the behavior of an electrodeposition reaction under conditions of pure diffusion control. Capacitive contributions to the current and electrolyte resistance effects are neglected. The deposition reaction is assumed to occur reversibly with the deposit at unit activity. Here in Part I, we treat the problem of a rotating disk electrode (RDE), and employ the Nernst-Siver approximation (3) for transient convective diffusion.

Even with the foregoing assumptions and perhaps the simplest electrochemical reaction, the complexity of the computational problem is still considerable, especially when the reaction occurs on an RDE under multi-sweep CV conditions. However, these assumptions enable one to obtain analytical expressions for most quantities of interest. With respect to the more general use of multi-sweep CV in electrodeposition, analysis of reversible deposition behavior is expected to exhibit the characteristic features of a pure diffusion control, and can thus serve

as a guide for treatment of more realistic deposition problems. Such problems will have to be treated numerically and the existence of a guide would be very helpful for the optimal manipulation of parameters.

It is shown from the analysis presented here that besides currents, methods exist for the computation of both the concentration of the reacting ion and the integral charge associated with the deposition process. This is achieved by the introduction of dimensionless current density, charge density, and concentration functions. It is shown that if the electrode potential, initially at equilibrium, is changed linearly in the cathodic direction for a time greater than the RDE characteristic time, then, upon cyclic potential reversal, all three functions become periodic with respect to time. In other words, periodicity is attained immediately after the first cathodic sweep provided that it extends beyond the RDE characteristic time.

The first cathodic sweep in multi-sweep CV is equivalent to linear sweep voltammetry (LSV). The LSV current response for reversible deposition of an RDE has already been described in the literature (4). The periodic cyclic voltammogram is significantly different from the LSV. For instance, the height of the cathodic maximum is reduced, the extent of this reduction depending on the dimensionless sweep rate. In addition, its position on the potential axis is not fixed. Whereas the first sweep begins at zero current, the foot of the periodic CV current wave exhibits a dependence on dimensionless sweep rate which is of diagnostic importance. Concentration functions during single and multi-sweep CV are shown to be complex, e.g. the existence of multiple concentration extrema into the electrolyte in the beginning of the periodic cathodic wave gives

rise to local mass fluxes away from both the electrode surface and the bulk electrolyte towards a depleted region within the boundary layer. However, concentration profiles are shown to provide physical insight towards understanding of the existence of a current maxima in multi-sweep CV. Finally, the charge density functions show that any complete CV sweep results in the formation of a net deposit on the electrode surface.

Definitions and Analysis

We begin our analysis by introducing dimensionless parameters. This is important not only because their number and range of variation is greatly systematized, but also because RDE behavior under CV conditions is described by a combination of dimensional sweep rate, v, and rotation speed, ω, rather than by each alone. This combination appears (4-7) in the definition of the dimensionless sweep rate.

$$\sigma = nFv\delta^2/RTD \qquad [1]$$

where δ is the thickness of the Levich diffusion layer, and D is the diffusion coefficient of the reacting ion. n, F, R, and T have their usual meaning. δ^2/D is the RDE characteristic time, defined once δ is fixed by the rotation speed. It should be noted that eq. [1] becomes obvious once one realizes that it is the simplest way to reduce v. Also, it should be emphasized that σ increases with increasing dimensional sweep rate, but decreases with increasing rotation speed. For example, at 100 rpm, $\sigma \sim 10$ when v = 100 mV/sec^{-1} in an electrolyte with $\nu = 10^{-2}$ $cm^2.sec^{-1}$ and $D = 10^{-5}$ $cm^2.sec^{-1}$ (n = 1, T = 25°C). However at 1000 rpm, σ drops to ~1 under the same conditions, and a sweep rate of 1 $volt.sec^{-1}$ is required to sustain its value at that rotation speed.

Dimensionless distance, time and concentration are defined by the following equations:

$$\xi = x/\delta \; ; \; \tau = Dt/\delta^2 \; ; \; C = 1-c/c^b \qquad [2]$$

where x is the distance away from the electrode surface, t is time, and c^b is the bulk (also initial) concentration of the reacting ion.

The dependence of the potential on dimensionless time is shown in Fig. 1a. The initial potential is the equilibrium, E_{eq}, computed from the Nernst equation on the basis of c^b. E_c is the cathodic reversal potential reached after a time of θ sec at a sweep rate of v volts.sec^{-1}; θ' is then a dimensionless reversal time defined by

$$\theta' = D\theta/\delta^2 \qquad [3]$$

Since the initial potential is E_{eq}, the interval E_c-E_{eq} is also one of cathodic overpotential varying from 0 to η_c, where η_c is the cathodic reversal overpotential. Figure 1b shows the dependence of the surface concentration on dimensionless time. When the potential is linearly dependent on time, the concentration is exponential through the Nernst equation. The list of dimensionless variables is extended by defining τ_c and τ_a. These are dimensionless times into a cathodic or anodic sweep, respectively. From Fig. 1a,

$$\tau = 2\ell\theta' + \tau c \; ; \; 0 \leqslant \tau_c \leqslant \theta' \; ; \; \tau \text{ during a cathodic sweep} \qquad [4a]$$

$$\tau = (2\ell+1)\theta' + \tau_a \; ; \; 0 \leqslant \tau_a \leqslant \theta' \; ; \; \tau \text{ during an anodic sweep} \qquad [4b]$$

Equations [4a] and [4b] are important in separating t in two components: the number of already applied complete cycles, ℓ, and time into a cathodic or anodic sweep, τ_c or τ_a, respectively.

We now focus on the definition and methods of computation of the concentration, current density, and charge density functions. Let us assume for the moment that a step potential is applied to the RDE such that the surface concentration becomes 0 at t=0 and remains at this value for all t>0. The solution of this problem, $C_s(\xi,\tau)$, is related to $C(\xi,\tau)$ by means of Duhamel's (or superposition) theorem (4,8,9):

$$C(\xi,\tau) = \int_0^\tau \frac{\partial C}{\partial \tau}(0,\lambda) \cdot C_s(\xi, \tau-\lambda)d\lambda \qquad [5]$$

where $C(0,\tau)$ is the time dependence of the surface concentration (Fig. 1b). According to the Nernst-Siver approximation,

$$C_s(\xi,\tau) = 1-\xi + 2\sum_{j=1}^{\infty} (-1)^j (j\pi)^{-1} \sin[(1-\xi)\, j\pi] \exp(-j^2\pi^2\tau) \qquad [6]$$

By combining eqs. [4], [5], and [6], expressions for the concentrations during a sweep can be derived (see Appendix). Apart from ξ, the concentrations will depend either on τ_c or on τ_a, depending on the direction of the potential sweep, and also on the parameters σ and θ'. We can then write $C_c^{\ell}(\xi,\tau_c;\sigma,\theta')$ for the dimensionless concentration during the $(\ell+1)^{th}$ cathodic sweep as a function of dimensionless time into the sweep, τ_c, distance, ξ, away from the electrode surface, dimensionless sweep rate, σ, and reversal time, θ'. The corresponding symbol for the concentration during the $(\ell+1)^{th}$ anodic sweep is $C_a^{\ell}(\xi,\tau_a;\sigma,\theta')$.

Once concentrations are available, currents can be computed from their ξ-derivative on the electrode surface. We define a current density function, J, as the dimensionless ratio of the current density to the diffusion limiting current density, i_L. The current density function during the $(\ell+1)^{th}$ cathodic cycle will depend on τ_c and on the parameters σ and θ'. We can thus represent it by $J_c(\tau_c;\sigma,\theta')$; similarly, we can use $J_a^{\ell}(\tau_a;\sigma,\theta')$ for the $(\ell+1)^{th}$ anodic cycle. J's can be computed either from

$$J_c^{\ell}(\tau_c;\sigma,\theta') = -\frac{\partial C_c^{\ell}}{\partial \xi}(o,\tau_c;\sigma,\theta') \; ; \; J_a^{\ell}(\tau_a;\sigma,\theta') = -\frac{\partial C_a^{\ell}}{\partial \xi}(o,\tau_a;\sigma,\theta') \quad [7]$$

or directly by Duhamel's theorem,

$$J = -\int_o^{\tau} \frac{\partial C}{\partial \tau}(o,\lambda) \cdot \frac{\partial C_s}{\partial \xi}(o,\tau-\lambda)d\lambda = \int_o^{\tau} \frac{\partial C}{\partial \tau}(o,\lambda) \cdot \theta_3(o,\pi i(\tau-\lambda))d\lambda \quad [8]$$

where the function θ_3 originates from differentiation with respect to ξ of eq. [6].

Since detailed expressions are available for the dependence of current on time, the charge deposited during a time interval can be computed. We define a charge density function, R, as the dimensionless ratio of the charge density deposited during a sweep to a characteristic charge density. The latter quantity is $i_{\ell}\delta^2/D$, i.e. the charge that would be deposited if the diffusion limiting current was applied for δ^2/D.

By definition, R's do not represent charge accumulation during repeated cycling but are specific to a particular cycle. The symbol $R_c^{\ell}(\sigma,\theta')$ will be used to denote the value of the charge density during the $(\ell+1)^{th}$ cathodic sweep as a function of dimensionless sweep rate and reversal time; similarly, for $R_a^{\ell}(\sigma,\theta')$. Apart from R_c and R_a, a third charge function is of particular significance:

$$R_n^{\ell}(\sigma,\theta') = R_c^{\ell} + R_a^{\ell} \quad [9]$$

R_n^{ℓ} represents the net cathodic ($R_n>0$) charge deposited during the complete $(\ell+1)^{th}$ sweep.

Expressions for the charge functions have been derived by integrating J's over time:

$$R_c^{\ell}(\sigma,\theta') = \int_o^{\theta'} J_c^{\ell}(\tau_c;\sigma,\theta')d\tau_c \; ; \; R_a^{\ell}(\sigma,\theta') = \int_o^{\theta'} J_a^{\ell}(\tau_a;\sigma,\theta')d\tau_a \quad [10]$$

Although $\theta' \geq 1$ is not a very important parameter in the computation of concentration and current density functions, its significance becomes decisive for R's. Since most electronic equipment available for electrochemical measurements control potential, it would be more useful to express R's as functions of reversal overpotential, η_c, rather than θ'. Expressing η_c as multiples of RT/nF, we may introduce a dimensionless overpotential, H, by

$$H = \eta/(RT/nF) \; ; \; H_c = \eta_c/(RT/nF) \qquad [11]$$

Expressions for $R_c^{o}(\sigma,H_c)$, $R_c(\sigma,H_c)$, $R_a(\sigma,H_c)$, and $R_n(\sigma,H_c)$ have been derived and are given in the Appendix.

Attainment of a Periodic State

It is shown in the Appendix that for

$$\theta' \geq 1 \; ; \; \theta \geq \delta^2/D \qquad [12]$$

all functions C_c^{ℓ}, C_a^{ℓ} ; J_c^{ℓ} ; J_a^{ℓ} ; R_c^{ℓ}, R_a^{ℓ} become independent of ℓ for all practical purposes. In other words, if the first cathodic wave (LSV) lasts for a time greater than δ^2/D, then all subsequent anodic waves are identical. Furthermore, the second and all subsequent cathodic waves are also identical. This is true irrespective of the value of the dimensionless sweep rate. The restriction on the value of θ' is not very serious since δ^2/D is usually a small quantity. However, one should be careful in realizing that the criterion for periodicity is time rather than reversal overpotential. For example, at a rotation speed of 100 rpm, δ^2/D ~ 2.5 sec. At a sweep rate of 1 volt·sec^{-1}, the reversal overpotential should be at least 2.5 volts for the periodicity criterion, eq. [12], to

be met. Conceivably, if $\theta' < 1$, letting $\ell \to \infty$ will give rise to a periodic state which will be in general different than the one established when eq. [12] is satisfied. In this paper, we analyze the periodic state arising from reversal times greater than the RDE characteristic time. Dimensionless periodic functions will be denoted by ℓ-independent symbols, and by using ≥ 1 instead of θ' for emphasis. For example, the periodic cathodic current density function will be $J_c(\tau_c; \sigma, \geq 1)$. It should be noted that periodic cathodic functions are independent of θ', so that its exact value is not of significance as long as it is ≥ 1.

Results and Discussion

We begin by discussing the periodic cathodic and anodic current density functions, $J_c(\tau_c; \sigma, \geq 1)$ and $J_a(\tau_a; \sigma, \geq 1)$. Contrary to stationary electrode behavior behavior, RDE voltammetry gives results which are parametrized with respect to σ alone, rather than combinations of $\sigma\tau$ and $\sigma\theta'$, a fact which renders direct correlations with overpotential impractical. It has been shown (4) that $J_c^{\circ}(\tau_c; \sigma)$, LSV current function, is a monotonically increasing function of τ_c, when $\sigma \lesssim 3$; also $J_c^{\circ}(o; \sigma) = 0$ and $J_c^{\circ}(\infty; \sigma) = 1$. In other words, on the first sweep, the initial value of the current is 0, in agreement with intuition, since the initial potential is the equilibrium potential, and for large τ_c values, the diffusion limiting current, i_L, is reached. For $\sigma \gtrsim 3$, a maximum in J_c° is observed. The reason for existence of this maximum will be explained in the discussion of the concentration profiles. Although the position of the maximum on the dimensionless time axis changes to lower τ_c values as σ increases, when $\sigma \gtrsim 4$, the maximum appears at the same location on the overpotential axis, equal to 0.854 (RT/nF) (= 22/n at 25°C). This is true only for J_c° for a reversible

deposition; reactions with finite kinetics (6) show a markedly different behavior. For large values of σ ($\sigma \gtrsim 4$) achieved by fast dimensional sweep rates, v, or low rotation speeds (eq. 1), or both, the role of convection becomes insignificant and RDE behavior becomes indistinguishable from stationary electrode behavior. This is so because in this range of σ values, LSV peaks appear at very short times, in which the concentration disturbance is limited to a small distance into the diffusion layer. Lack of rotation speed dependence renders the value of the J_c° maximum a linear function of $\sigma^{1/2}$ with a slope of 0.61. It should be noted that $\sigma^{1/2}$ is the only dependence which eliminates δ(thus ω) from the combination $i_L\sigma^{1/2}$.

Upon multiple sweeping, the behavior of the periodic currents is markedly different from those obtained by LSV (Fig. 2). This is expected since periodicity means relatively large times at which convective effects are fully operational. An important feature of the periodic cathodic current function is that a portion of it near its foot is anodic, i.e. substrate dissolution rather than deposition occurs. The tail of the periodic current during the anodic sweep is also anodic. The periodic cathodic current does not exhibit a peak for $\sigma \lesssim 3$. For higher σ values, a maximum appears, which has the same physical origin as the LSV maximum; the origin of these maxima are discussed in the analysis of concentration profiles. As expected, the periodic anodic current function is always monotonic, since no conceivable limitation on the dissolution reaction exists. As will be seen later, the amount of deposit dissolved during a cycle in which the current is anodic never exceeds the amount deposited during the same cycle when the current is cathodic. By performing a multi-sweep experiment then, one does not run into the danger of dissolving the

initial electrode substrate. However, this should initially be of the same materials as the reaction product, to guarantee the definition of the equilibrium potential as well as to satisfy the assumption of constant deposit activity.

The general shape of the periodic current density functions indicates that there are three criteria of diagnostic importance. These are: the dependence of the value of the foot of the cathodic sweep current (an anodic current) on σ; the dependence of the location and height of the cathodic current maxima on σ. Two properties of the current density functions should be emphasized. The absence of an extremum in the periodic anodic current renders such considerations as maxima separation on the time (or potential) axis inapplicable, and the expressions for J_c are independent of θ' provided that eq. [12] is satisfied. That is why the quantities of diagnostic importance are defined only by σ and not by σ and θ'. Since the periodic anodic function assumes virtually the same values as the cathodic function at its foot and tail, it follows that it also exhibits an insignificant dependence on θ' at these points.

The dependence of J_c on σ at $\tau_c=0$ is described by the following relation:

$$J_c\,(0;\ \sigma,\geqslant 1) = J_a\,(\theta';\ \sigma,\geqslant 1) = 1-\sigma^{1/2}\coth(\sigma^{1/2})^{\dagger} \qquad [13]$$

This equation shows that $J_c(0)$ is always negative (anodic current) and that its value can become significantly higher than -1 depending on σ, i.e. several multiples of i_L can be measured in the anodic current region

---

†Application of de l'Hôpital's rule shows that this expression has a finite limit as $\sigma\to 0$; i.e. $\lim_{\sigma\to 0} J_c = 0$, despite $\lim_{\sigma\to 0} \coth(\sigma^{1/2}) = \infty$.

(Fig. 2). For $\sigma \geqslant 9$, eq. [13] can be simplified

$$J_c\ (0; \geqslant 9, \geqslant 1) = 1-\sigma^{1/2} \qquad [14]$$

The height of the maximum in the periodic current function ($\sigma \gtrsim 3$) is significantly lower than in LSV; whereas,

$$J_c^{\circ}{}_{,max} = 0.61\ \sigma^{1/2}\ ;\ \sigma \geqslant 4 \qquad [15]$$

a numerical correlation indicates that

$$J_{c,max} = 0.881\ \sigma^{0.251} \sim 0.881\ \sigma^{1/4}\ ;\ \sigma \geqslant 9 \qquad [16]$$

Values of $J_{c,max}$ in the range $3<\sigma<9$ are reported in Table 1. It should be noted that as σ increases, the difference between $J_{c,max}^{\circ}$ and $J_{c,max}$ also increases. $J_{c,max}$ appears at generally higher cathodic overpotentials than $J_{c,max}^{\circ}$; whereas

$$H^{\circ}_{max} = 0.854\ ;\ \sigma \geqslant 4 \qquad [17]$$

in the case of periodic current functions,

$$H_{max} \cong 1.3 - 1.4\ ;\ \sigma \geqslant 9 \qquad [18]$$

It should be pointed out that like eq. [16], eq. [18] is a numerical result, the validity of which has been investigated in the range $9<\sigma<50$.

We conclude our discussion on current density functions during LSV and multi-sweep CV by an analysis of their behavior in terms of dimensional times and potentials. To this effect, a single electron reversible deposition reaction is chosen (n=1) occurring on a RDE with ω = 100 rpm

at 25°C from an electrolyte with $\nu = 10^{-2}$ cm^2·sec^{-1}; the diffusion coefficient of the depositing ion is assumed to be equal to 10^{-5} cm^2·sec^{-1}. With these data, the RDE characteristic time is ~2.5 sec. Figure 3a shows the dependence of J_c° (LSV current function) on dimensional time, for various values of the dimensional sweep rate. At v = 20 mV·sec^{-1}, σ~1.9 and no maximum appears. When v = 100 mV·sec^{-1} (σ~9.6), the maximum appears at ~0.21 sec and its height is described by eq. [15]. At 300 mV·sec^{-1} (σ~28.9), the maximum appears at a much shorter time of ~0.07 sec. An interesting feature of Fig. 3a is that the time necessary for the attainment of the limiting current (J_c°=1) decreases with increasing sweep rate (10). It would thus seem advantageous to use as high a sweep rate as possible if the aim of the experiment is the measurement of i_L.

In order to attain periodic behavior in subsequent sweeps, the LSV sweep should last for at least 2.5 sec, in accordance with eq. [12]. In terms of overpotential, one would have to apply at least 750 mV when v = 300 mV·sec^{-1}, as opposed to 50 mV if v = 20 mV·sec^{-1}.† Figure 3b shows the LSV and periodic cathodic current functions plotted vs. cathodic overpotential. It is clearly seen that as v increases, the difference in height between $J_{c,max}^\circ$ and $J_{c,max}$ also increases. When v = 20 mV·sec^{-1}, J_c° and J_c differ only around η_c = 0. The overpotential at the maximum for all LSV curves is 22 mV, whereas for the periodic curves it is ~35 mV; also, $J_{c,max}$ for 300 mV·sec^{-1} is slightly displaced towards more cathodic overpotentials as compared to the one at 100 mV·sec^{-1}. With respect to

†The exact value of D may be very significant with respect to these considerations.

limiting currents, higher overpotentials are required to attain i_L. It becomes obvious that although smaller times are required for the measurement of i_L, the combined time-sweep rate effect gives rise to the opposite behavior in terms of overpotential, i.e. for faster sweeps, a higher overpotential must be applied for the current to reach the i_L value. Since in many situations undesirable reactions may occur concurrently with the deposition process, the choice of sweep rate in the potentiodynamic determination of i_L should result from a balance between times and overpotentials.

We now turn our attention to the concentration profiles which develop into the electrolyte during a multi-sweep CV experiment on a RDE. These are drawn in Figs. 4 and 5 from expressions for LSV and periodic CV concentrations developed in the Appendix. Two representative values of σ are used, 6 and 1, chosen by the presence or absence of a maximum in J_c° and J_c. Figures 4a and 5a are the current functions for these values of σ. In all other figures, the function $1-C(\xi, \tau;\sigma,\theta') = c/c^b$ instead of $C(\xi, \tau;\sigma,\theta') = 1- c/c^b$ is plotted. Since the surface concentration (ξ=o) decreases from c^b to $c^b \exp(-\sigma\theta')$ during a cathodic sweep and increases from $c^b \exp(-\sigma\theta')$ to σ^b during an anodic sweep, the function c/c^b changes from 1 to $\exp(-\sigma\theta')$ and from $\exp(-\sigma\theta')$ back to 1. For a given value of τ_c or τ_a, the derivative of the concentration curve evaluated at the surface (ξ=o) yields the value of J at that time.

Figure 4b refers to curve (a) in Fig. 4a. Concentration curves bend continuously and their ξ-derivative at ξ=o is in the same direction, since the current is always cathodic. Curve (c) is nearest to the cathodic maximum. Comparison of curve (c) with (b) and (d) indicates

that the appearance of a maximum in J_c° is related to the curvature of the concentration profile into the electrolyte. It appears that the rate by which concentration changes at $\xi>o$ cannot match the rate of variation at $\xi=o$. This curvature gives rise to transient currents higher than i_L, despite the non-zero value of the concentration. When sufficient time passes, the whole profile comes closer to being linear, the curvature at $\xi=o$ decreases and consequently, the cathodic current also decreases. As shown by line (f), Fig. 4b, the concentration profile is almost linear at $\tau_c=1$.

When the first - also periodic - anodic cycle begins, Fig. 4a(c), the concentration profile is almost linear ($i\sim i_L$)(curve (f) in Figs. 4b and 4c) and the current is cathodic. The current remains cathodic for the time interval $0<\tau_a<0.85$. When $\tau_a = 0.85$, $J_a = 0$ as witnessed by a 0 derivative at $\xi=0$ for curve (d) in Fig. 4c. For $\tau_a>0.85$, the current is anodic and an inevitable concentration extremum is formed into the electrolyte, which is most pronounced when $\tau_a = 1$. The existence of this extremum can be predicted without a formal solution of the diffusion problem, since it is the only possibility which can simultaneously satisfy three requirements; that the current be anodic (surface derivative pointing downwards); that the concentration at $\xi=o$ vary between c^b and ca. 0 only; and that the concentration at $\xi=1$ be fixed at c^b (according to the boundary condition imposed by the Nernst-Siver approximation).

In the beginning of the second - also periodic - cathodic sweep, the concentration profile has a complicated shape (curve (a) in Figs. 4c, d, e). At the same time, the surface concentration changes rapidly. The

inability of the concentration into the electrolyte to match the rapidity of the surface concentration change results in a complex regime of mass fluxes shown in Figs. 4e and 4d (exploded version of the early stages of 4e). Curvature readjustments can now explain both the existence of a maximum in the periodic cathodic current function and the fact that it is lower in height and delayed in time.

Apart from Figs. 4a and 5a, the differences between Figs. 4 and 5 are mostly of quantitative than qualitative nature. Curve (d) in Fig. 5b clearly shows that at the chosen low value of the dimensionless sweep rate, the value of the current is far from i_L when $\tau_c=1$, despite the fact that the periodicity criterion, eq. [12], is met. Finally, the concentration extremum is less intense during the periodic anodic sweep, resulting in faster readjustment during the following periodic cathodic sweep.

We conclude our discussion with an analysis of results pertaining to the charge density functions. These are drawn in Figs. 6a-c and Figs. 7a-b. Figure 6 illustrates the dependence of R's on σ and θ', whereas Fig. 7 on σ and H_c. The abscissa in Fig. 6 has been chosen with the purpose of contracting the scale of possible σ values. Apart from this, R_c° depends linearly on σ^{-1} for large values of σ; the periodic charge functions are ultimately linear in $\sigma^{-1/2}$. Although both Figs. 6 and 7 describe the same functions, they differ in their potential experimental determination. In Fig. 6, each cycle has a fixed time duration; in Fig. 7, what is implicitly fixed is the reversal overpotential. In view of the paramount significance of θ' in determining the value of the charge density functions, this difference is extremely important: it accounts for the fact that the charge increases with increasing dimensionless

sweep rate when θ' is fixed, whereas it decreases with increasing sweep rate when H_c is fixed. It is widely known from single sweep CV theory on stationary electrodes that charge is inversely proportional to dimensional sweep rate (usually its square root). Since charge functions for stationary electrodes usually depend on $(nF/RT)v\theta$, it is implied in this statement that, during the experiment, the reversal overpotential, $v\theta$, is fixed and v is varied. It seems that emphasizing experimental conditions in RDE theory is necessary, mainly because of the dependence of relevent CV functions on both σ and $\sigma\theta'$. It is appropriate here to recall that σ increases not only as a result of increasing sweep rate but also of decreasing rotation speed. It is intuitively expected that when both reversal overpotential and dimensional sweep rate are fixed, less charge should be deposited as the rotation speed decreases.

For a fixed θ', it is interesting to compare the values of the charge density functions with the charge that would be obtained, were the current constant and equal to i_L continuously during the performance of the experiment (interrupted lines, Figs. 6a-c). In the range of σ values of electroanalytical significance ($\sigma \geq 3$), it is seen that the values of the charge functions are primarily determined by θ'. This is expected since the dimensionless time interval during which the current is different than i_L is increasingly shorter as σ increases. It follows that the range of σ in which R's change significantly is below the value for which the cathodic current maximum appears.

Since the current density during an anodic cycle is always below the corresponding value for the cathodic cycle when both are cathodic and the opposite when they are anodic, it is expected that the periodic anodic

charge density will always be lower than the periodic cathodic (Fig. 6b). It turns out that for $\theta' \geq 1$, it is also positive irrespective of σ, indicating that during any periodic anodic cycle a net deposit is added to the electrode. Obviously, the net charge density function, R_n (Fig. 6c) is also positive, indicating that a complete cycle always results in the formation of a net deposit. Similar conclusions can be drawn for the first sweep as well, since $R_c^\circ > R_c$ always. Interestingly, for very large values of σ, the interval over which the current is different from i_L is very narrow; in the limit of $\sigma \to \infty$, both periodic R_c and R_a tend to θ' and R_n to $2\theta'$. With respect to Fig. 6c, it is important to note that $R_n < 2\theta'$ for all finite σ. In other words, the amount of deposit obtained by plating with a non <u>dc</u> potential as in Fig. 1, can never exceed the amount obtained by dc plating at the limiting current, i_L. This result is in agreement with conclusions drawn from the study of pulsed currents (1). The present results are rigorously valid only for deposition reactions with infinitely fast kinetics. Since the LSV currents do not have anodic portions, it is possible that R_c° can exceed θ' as seen in Fig. 6a. Interestingly, the excess $R_c^\circ = \theta'$ is always less than 1/3 for finite σ and is independent of θ'.

Figure 7a is a plot of R vs. H_c for two representative σ values, 1 and 7. The range of H_c, $4 \leq H_c \leq 40$ for n=1 corresponds to approximately 100-1000 mV. For $H_c \geq 4$, the dependence of R on H_c is linear to a good approximation. Note that for $\sigma = 7$, the periodic charge density functions are drawn for $H_c \geq 7$, to satisfy eq. [12]. No such restriction exists for R_c°, for all σ. For $\sigma = 1$, eq. [1] is satisfied for all $H_c \geq 4$. Figure 7b emphasizes an interesting mathematical observation, namely, that the

function, R_n'

$$R_n'(H_c) = \sigma R_n(\sigma, H_c) = 2[H_c + \exp(-H_c) - 1] \; ; \; R_n(\sigma, H_c) = 2\sigma^{-1}[H_c + \exp(-H_c) - 1] \qquad [20]$$

is a function of reversal overpotential alone. For $H_c \geq 4$, it is also linear in H_c. Alternatively, for a fixed H_c, R_n is inversely proportional to σ, indicating linear dependence on the rotation speed ω, and on the inverse of the dimensional sweep rate, v. When both ω and v are varied so that σ is the same for each combination, R_n becomes independent of ω or v alone. This result emphasizes the fact that CV on a RDE is described by a combination of v and ω as it appears in σ, eq. [1], rather than each alone. In connection to Fig. 7a one should note that for $\sigma=1$, R_c^o, R_c, and R_a are close to each other; their separation increases with increasing σ but in each case there is a maximum for $\sigma \to \infty$.

Conclusions

It has been demonstrated that multi-sweep CV on a RDE leads to the establishment of a periodic response in concentrations, currents, and charges provided that the duration of each cycle is of the order of the RDE characteristic time. The first cathodic (LSV) sweep is the only one which is not periodic. Since this result originates from the study of reversible deposition reactions, its validity for other mechanisms can only be provisional.

The existence of a quickly attainable periodic state is significant in two respects. From the mathematical viewpoint, it indicates that the computational effort involved in the treatment of complicated reaction mechanisms need not be as great as one may originally think. From

the electroanalytical viewpoint, the periodic currents and charges offer information of diagnostic importance, in addition to that obtained from LSV data. Experimentally, this is equivalent to the recording of two sweeps in each case, instead of only the first. However, one should be cautious in interpreting multi-sweep periodic data: the dependence of the current functions is not as strong as in LSV. In addition, the prolonged existence of the complicated mass flux regimes arising during CV experiments may lead to undesirable effects. Clearly more experimental and computational work must be done in order for the screening capacibilities of the LSV-RDE and CV-RDE techniques to be ascertained on the quantitative level.

Acknowledgment

This work was supported by the Assistant Secretary for Conservation and Renewable Energy, Office of Advanced Conservation Technology, Division of Electrochemical Systems Research of the US Department of Energy under contract #DE-AC03-76SF00098.

Portions of this paper were presented at the 162nd Meeting of the Electrochemical Society, Detroit, Michigan, October 17-21, 1982, Abstract No. 322.

List of Symbols

B_j	coefficient; ref. 8
c	concentration
c^b	bulk concentration
C	dimensionless concentration; eq. [2]
$\overline{C}$	Laplace transform of C
C_s	dimensionless concentration obtained when an infinite potential step is applied to an RDE for a reversible deposition reaction; eq. [6]
$\overline{C}_s$	Laplace transform of C_s
C_a	periodic dimensionless concentration during an anodic sweep; eq. [A16]
C_c	periodic dimensionless concentration during a cathodic sweep; eq. [A15]
C_a^o	dimensionless concentration during the first anodic sweep; eq. [A12]
C_c^o	dimensionless concentration during LSV sweep; eq. [A11]
C_a^ℓ	dimensionless concentration during (ℓ+1)th anodic sweep; eq. [A14]
C_c^ℓ	dimensionless concentration during (ℓ+1)th cathodic sweep; eq. [A13]
C_{j_1}	coefficient; ref. 13
D	diffusion coefficient
E_{eq}	equilibrium potential
E_c	reversal potential
H	dimensionless overpotential; eq. [11]
H_c	dimensionless reversal overpotential; eq. [11]
H_{max}	value of H at the maximum of the periodic current density function

H^o_{max}	value of H at the maximum of the LSV current density function
i	current density
i_s	current response of an RDE to which an infinite potential step is applied for a reversible deposition reaction; eqs. [A19], [A51], [A52]
i_L	diffusion limiting current density
j	summation index
j_1	summation index
J_a	periodic anodic current density function; eq. [A27]
J_c	periodic cathodic current density function; eq. [A26]
J^o_a	current density function during the first anodic sweep; eq. [A23]
J^o_c	LSV current density function; eq. [A22]
J^ℓ_a	current density function during the (ℓ+1)th anodic sweep; eq. [A25]
J^ℓ_c	current density function during the (ℓ+1)th cathodic sweep; eq. [A24]
$J_{c,max}$	maximum value of J_c
$J^o_{c,max}$	maximum value of J^o_c
ℓ	number of applied complete potential cycles
p	Laplace parameter
R_a	periodic anodic charge density function; eqs. [A34],[A47]
R_c	periodic cathodic charge density function; eqs. [A33],[A46]
R_n	periodic net charge density function; eqs. [A35],[A48]
R^o_c	charge density function during the LSV sweep; eqs. [A32], [A45]

R_a^{ℓ}	charge density function during the (ℓ+1)th anodic sweep; eq. [A31]
R_c^{ℓ}	charge density function during the (ℓ+1)th cathodic sweep; eq. [A30]
R_n^{ℓ}	net charge density function during the complete (ℓ+1) sweep; eq. [9]
R_n'	defined by eqs. [20],[A49]
$R_{c,max}$	maximum value of R_c
t	dimensional time
v	dimensional sweep rate
x	dimensional distance away from RDE surface
δ	thickness of the Levich diffusion layer
ε	$\Gamma(4/3)$; eq. [A51]
ζ	dimensionless distance; ref. 8
η	overpotential
η_c	cathodic reversal overpotential
θ	reversal time
θ'	dimensionless reversal time; eq. [3]
λ	dummy variable of integration
λ_j	eigenvalue; ref. 8
λ_{j_1}	eigenvalue; ref. 13
ν	electrolyte kinematic viscosity
ξ	dimensionless distance; eq. [2]
σ	dimensionless sweep rate; eq. [1]

τ	dimensionless time; eq. [2]
τ_a	dimensionless time into an anodic sweep; eq. [4b]
τ_c	dimensionless time into a cathodic sweep; eq. [4a]
ω	RDE rotation speed

References

1. H. Y. Cheh, J. Electrochem. Soc., 118, 551 (1971).
2. T. R. Rosebrugh and W. L. Miller, J. Phys. Chem., 14, 816 (1910).
3. Yu. G. Siver, Russ. J. Phys. Chem., 33, 533 (1959); 34, 273 (1960).
4. P. C. Andricacos and H. Y. Cheh, J. Electrochem. Soc., 127, 2153 (1980).
5. P. C. Andricacos and H. Y. Cheh, J. Electrochem. Soc., 127, 2385 (1980).
6. P. C. Andricacos and H. Y. Cheh, J. Electroanal. Chem., 124, 95 (1981).
7. G. P. Girina, V. Yu. Filinovskii, and L. G. Feoktistov, Soviet Electrochem., 3, 831 (1967).
8. K. Nisangiolu and J. Newman, J. Electroanal. Chem., 50, 23 (1974).
9. P. C. Andricacos and H. Y. Cheh, J. Electroanal. Chem., 121, 133 (1981).
10. J. R. Selman and C. W. Tobias, J. Electroanal. Chem., 65, 67 (1975).
11. E. T. Whittaker and G. N. Watson, A Course of Modern Analysis, Cambridge University Press, London, 1969.
12. L. S. Gradshteyn and I. M. Ryzhic, Table of Integrals, Series and Products, Academic Press, New York, 1980.
13. K. Viswanathan, M. A. Farrell-Epstein and H. Y. Cheh, J. Electrochem. Soc., 125, 1772 (1978); K. Viswanathan and H. Y. Cheh, J. Appl. Electrochem., 9, 537 (1979).

Table 1. Values of $J_{c,max}$ in the Interval $3<\sigma<9$.

σ	$J_{c,max}$
3	1.059
4	1.176
5	1.274
6	1.354
7	1.421
8	1.478
9	1.528

Figure Captions

Fig. 1 Dependence of electrode potential and surface concentration on dimensionless time during multi-sweep cyclic voltammetry.

a. Electrode potential

b. Surface concentration for a reversible deposition reaction (Nernst equation).

Fig. 2 Periodic Current density functions in terms of dimensionless time; numbers on curves are values of the dimensionless sweep rate; in Fig. 2b anodic current functions have been omitted.

Fig. 3a LSV current density function in terms of dimensional time for various values of the dimensional sweep rate.

Fig. 3b LSV (solid lines) and Periodic (interrupted lines) cathodic current density functions in terms of cathodic overpotential for various values of the dimensional sweep rate. All solid lines begin at 0. Interrupted lines begin at some anodic value of the current which can be computed by eq. [13].

Fig. 4a Current density functions for $\sigma=6$.

a. $J_c^{\circ}(\tau_c;6)$ - LSV sweep (begins at zero)

b. $J_a(\tau_a;6,1)$ - periodic anodic

c. $J_c(\tau_c;6,1)$ - periodic cathodic

Fig. 4b Dimensionless concentration profiles within the Levich diffusion layer during the LSV sweep for $\sigma=6$. Corresponds to curve (a) of Fig. 4a.

Fig. 4c As in Fig. 4b, but during the first - also periodic - anodic sweep. Corresponds to curve (b) of Fig. 4a.

Fig. 4d As in Fig. 4b, but during the initial stages of the second - also periodic - cathodic sweep. Corresponds to curve (c) of Fig. 4a.

Fig. 4e As in Fig. 4b, but during the second - also periodic - cathodic sweep. Corresponds to curve (c) of Fig. 4a.

Fig. 5a As in Fig. 4a, but for $\sigma=1$.

a. $J_c^{\circ}(\tau_c;1)$

b. $J_a(\tau_a;1,1)$

c. $J_c(\tau_c;1,1)$

Fig. 5b As in Fig. 4b, but for $\sigma=1$.

Fig. 5c As in Fig. 4c. Corresponds to curve (b) of Fig. 5a.

Fig. 5d As in Fig. 4e. Corresponds to curve (c) of Fig. 5a.

Fig. 6a Charge density functions during the LSV sweep in terms of dimensionless sweep rate for various values of dimensionless reversal time.

1: $R_c^{\circ}(\sigma,2)$; 2: $R_c^{\circ}(\sigma,6)$; 3: $R_c^{\circ}(\sigma,10)$

Fig. 6b Charge density functions during the periodic cathodic and anodic sweeps.

1: $R_a(\sigma,1)$, 2: $R_c(\sigma,1)$; 3: $R_a(\sigma,6)$, 4: $R_c(\sigma,6)$;
5: $R_a(\sigma,10)$; 6: $R_c(\sigma,10)$

Fig. 6c Net charge density functions.

1: $R_n(\sigma,1)$; 2: $R_n(\sigma,6)$; 3: $R_n(\sigma,10)$.

Fig. 7a Charge density functions in terms of dimensionless cathodic overpotential

1: $R_c^{\circ}(1,H_c)$; 2: $R_c(1,H_c)$; 3: $R_a(1,H_c)$; 4: $R_n(1,H_c)$
5: $R_c^{\circ}(7,H_c)$; 6: $R_c(7,H_c)$; 7: $R_a(7,H_c)$; 8: $R_n(7,H_c)$

Fig. 7b Dependence of the σ-independent combination $R'_n = \sigma R_n$ in terms of dimensionless cathodic overpotential.

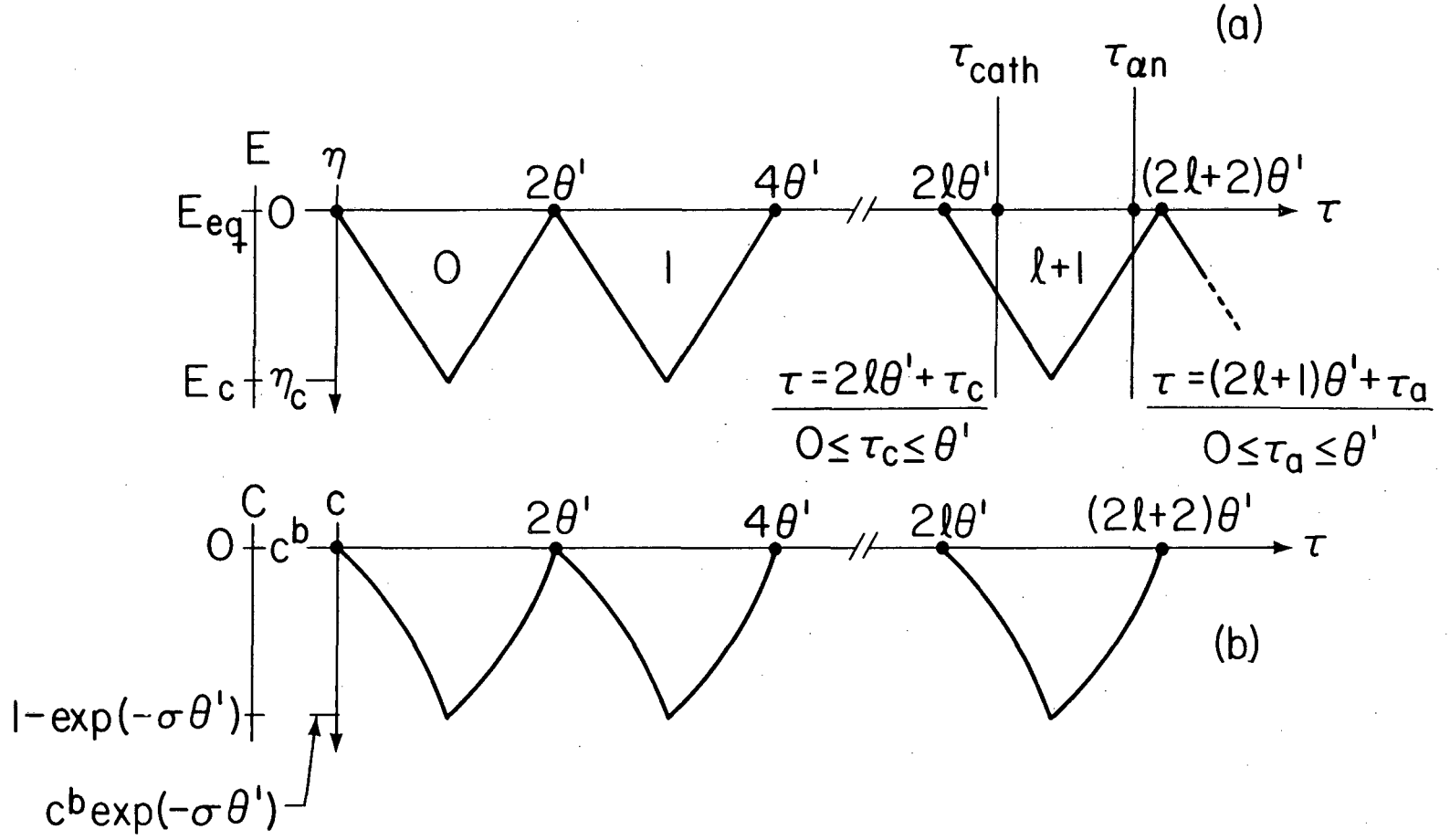

XBL 825-629

Fig. 1

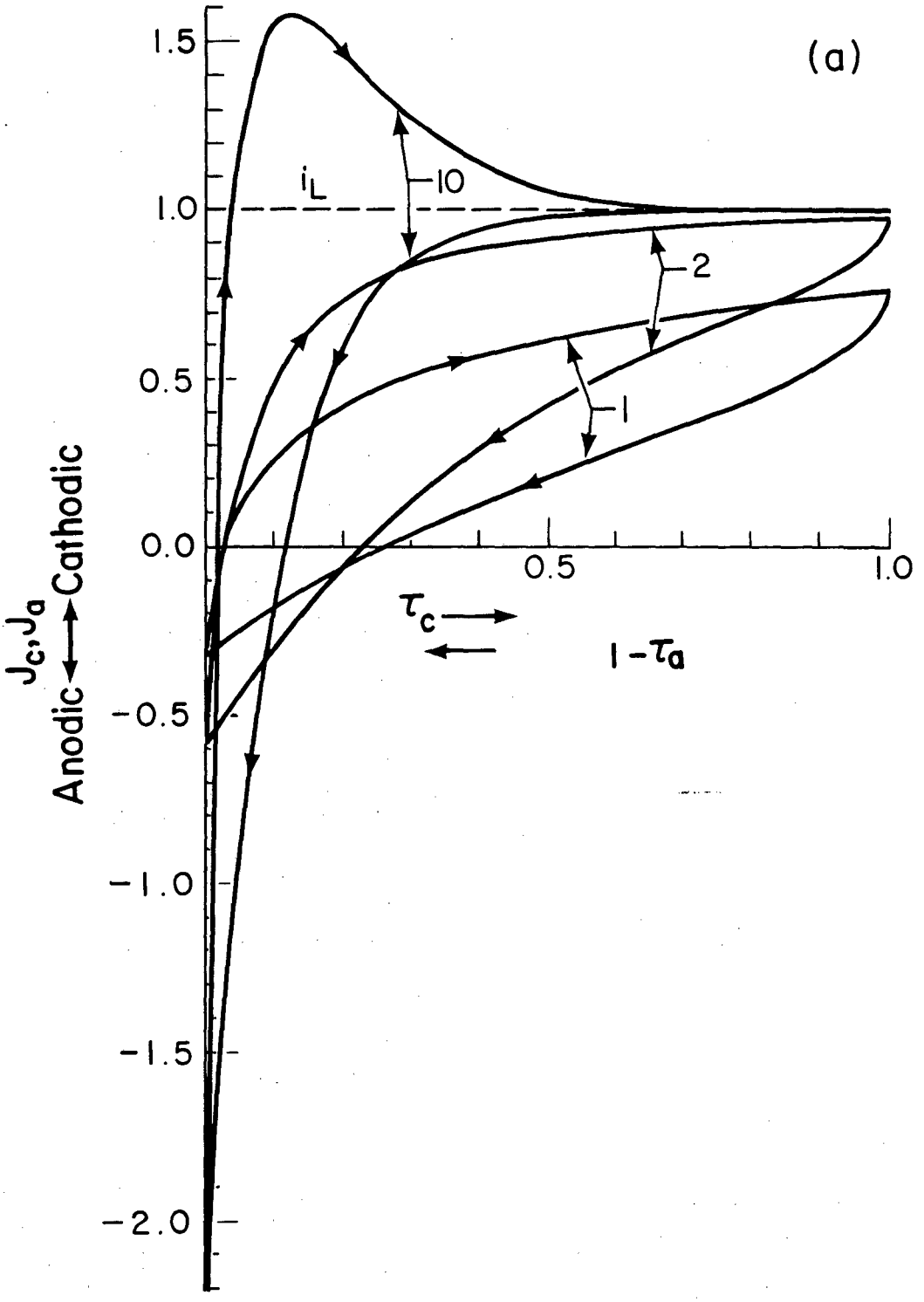

XBL 825-620

Fig. 2a

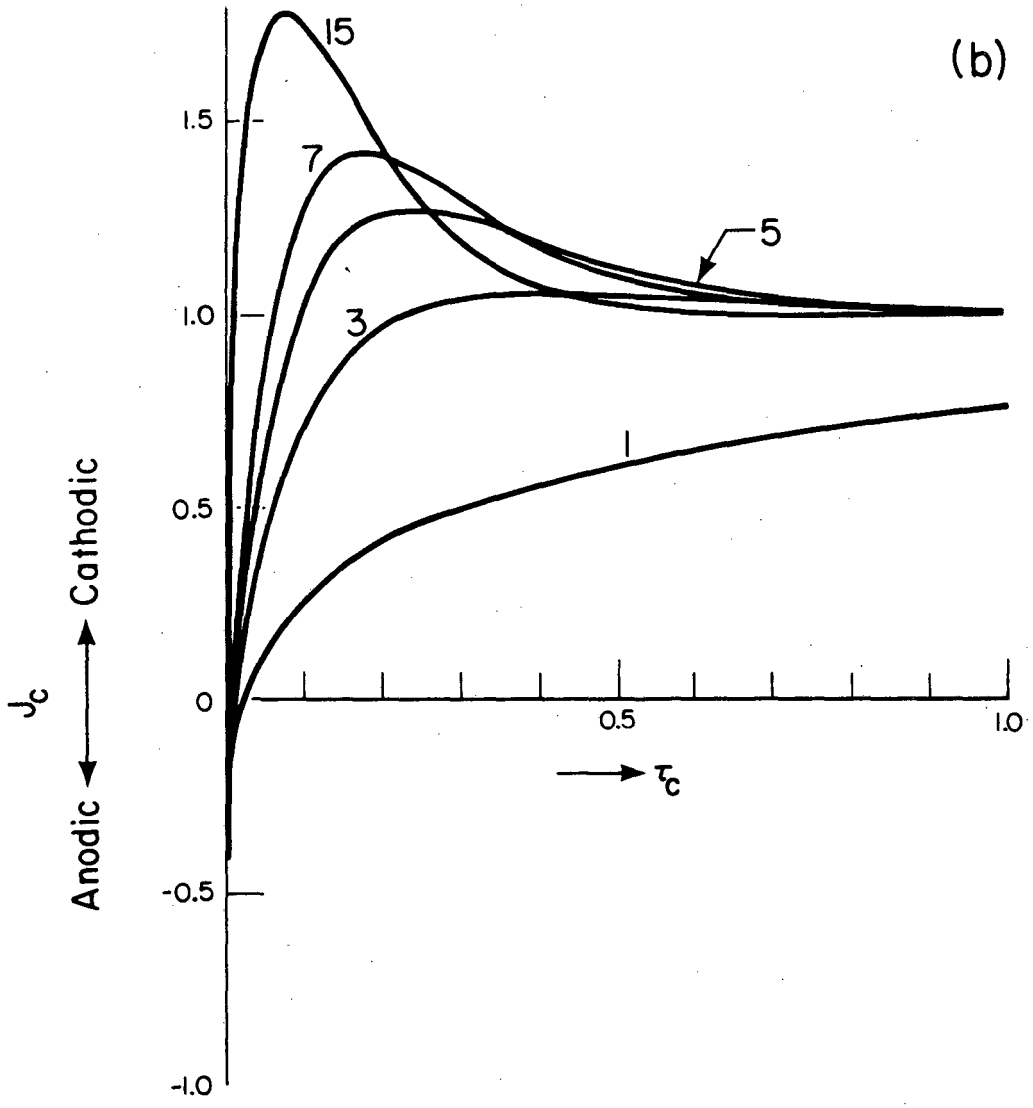

XBL 825-625

Fig. 2b

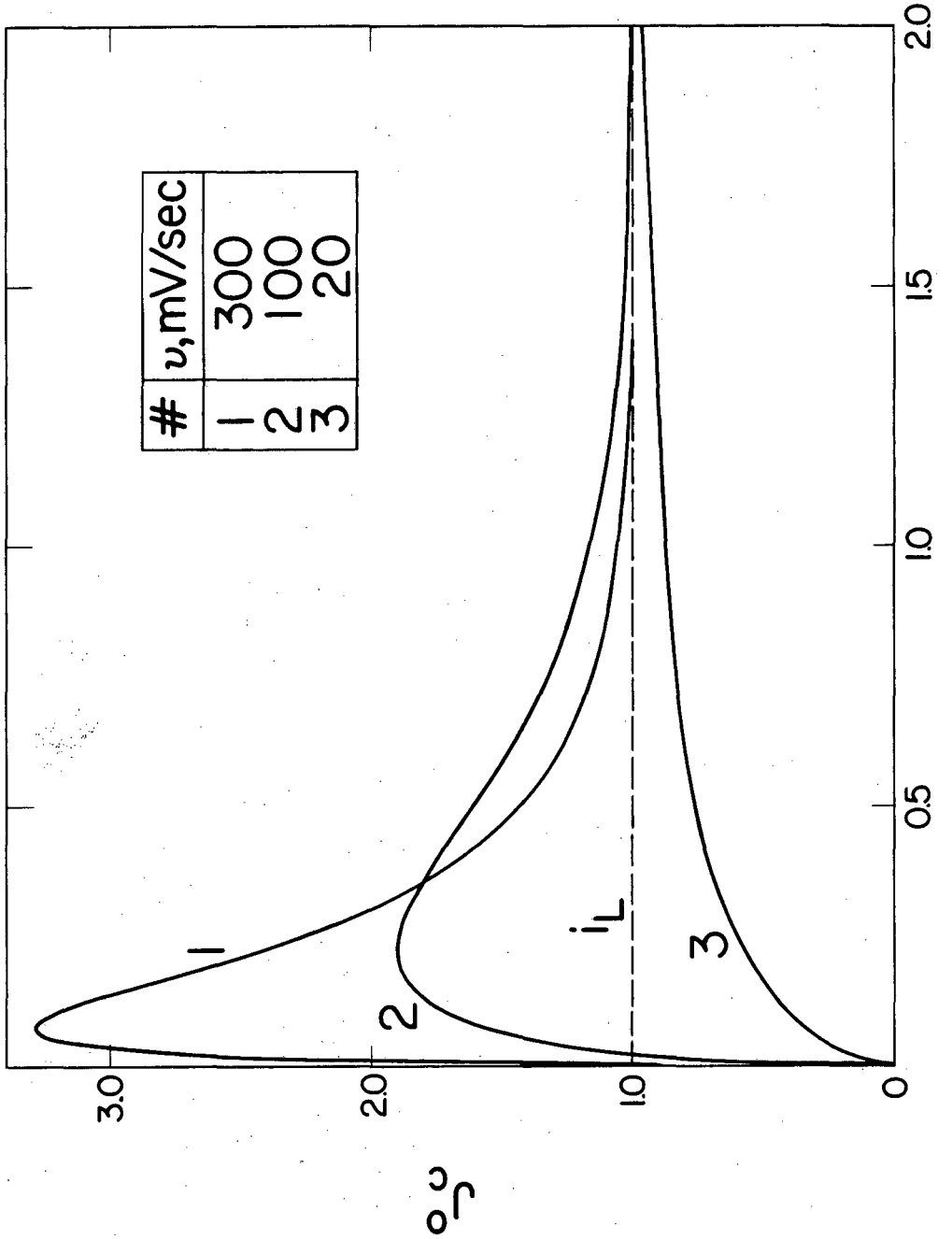

XBL 825-634

Fig. 3a

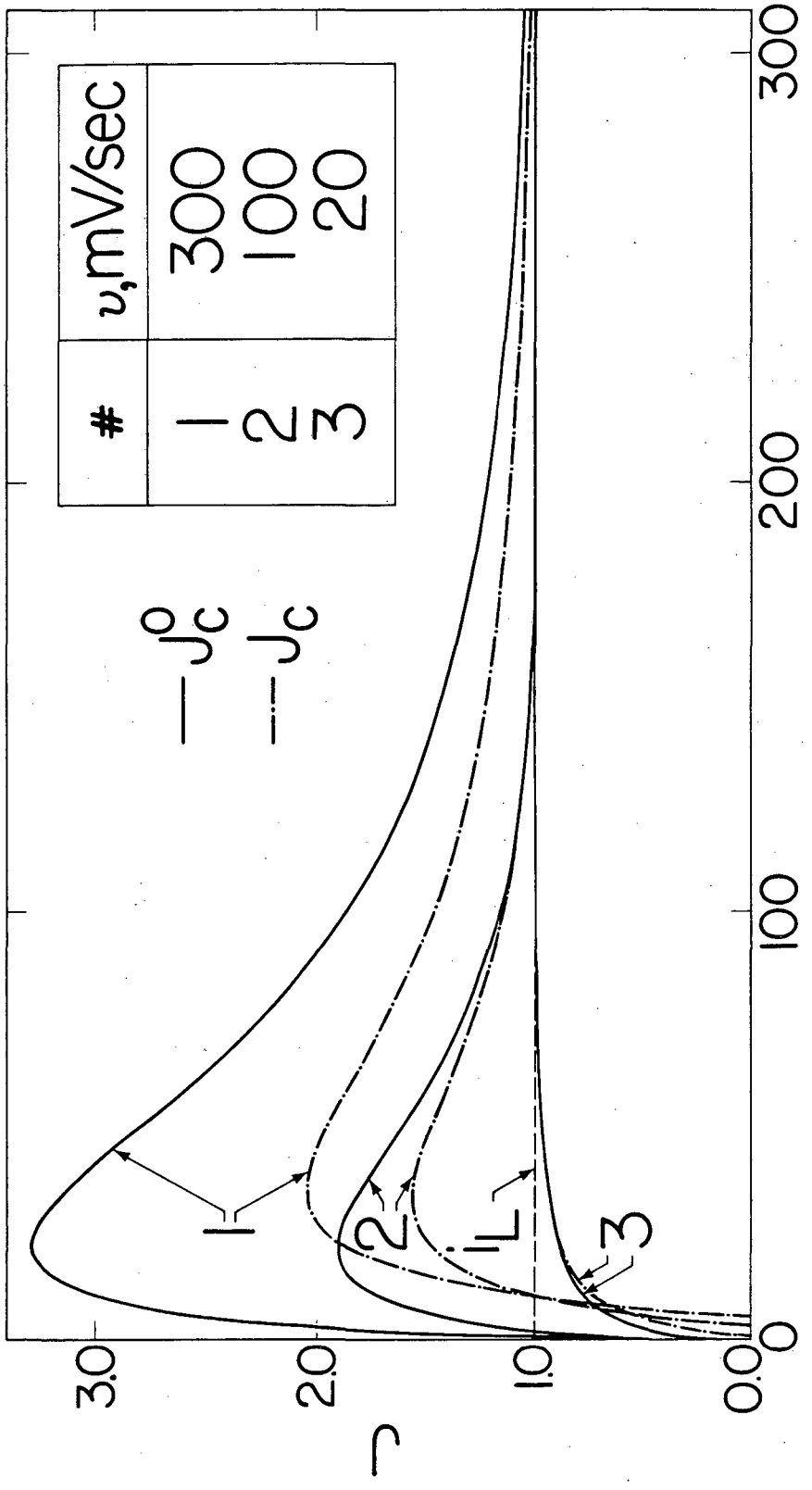

XBL 825-638

Fig. 3b

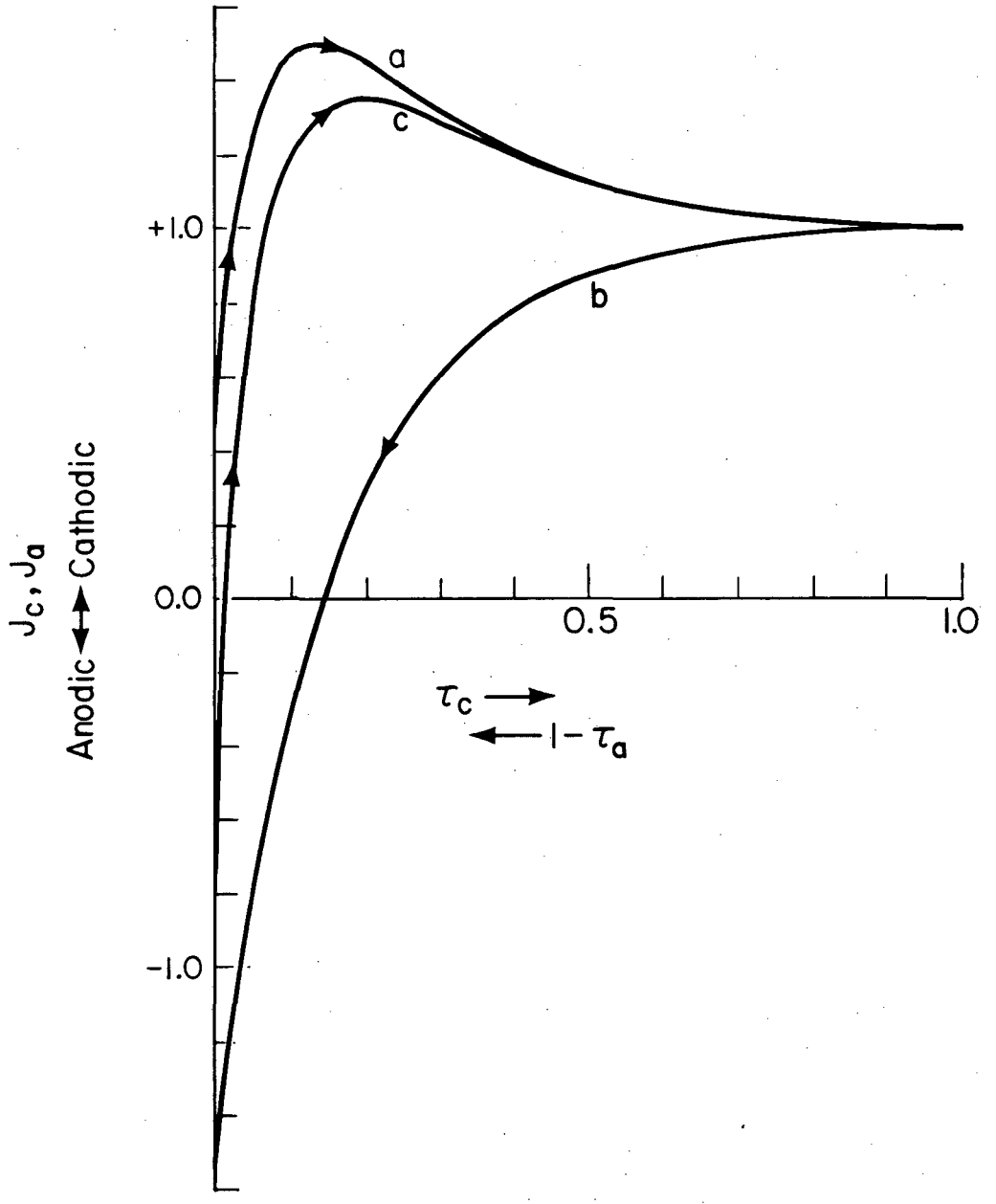

XBL 825-627

Fig. 4a

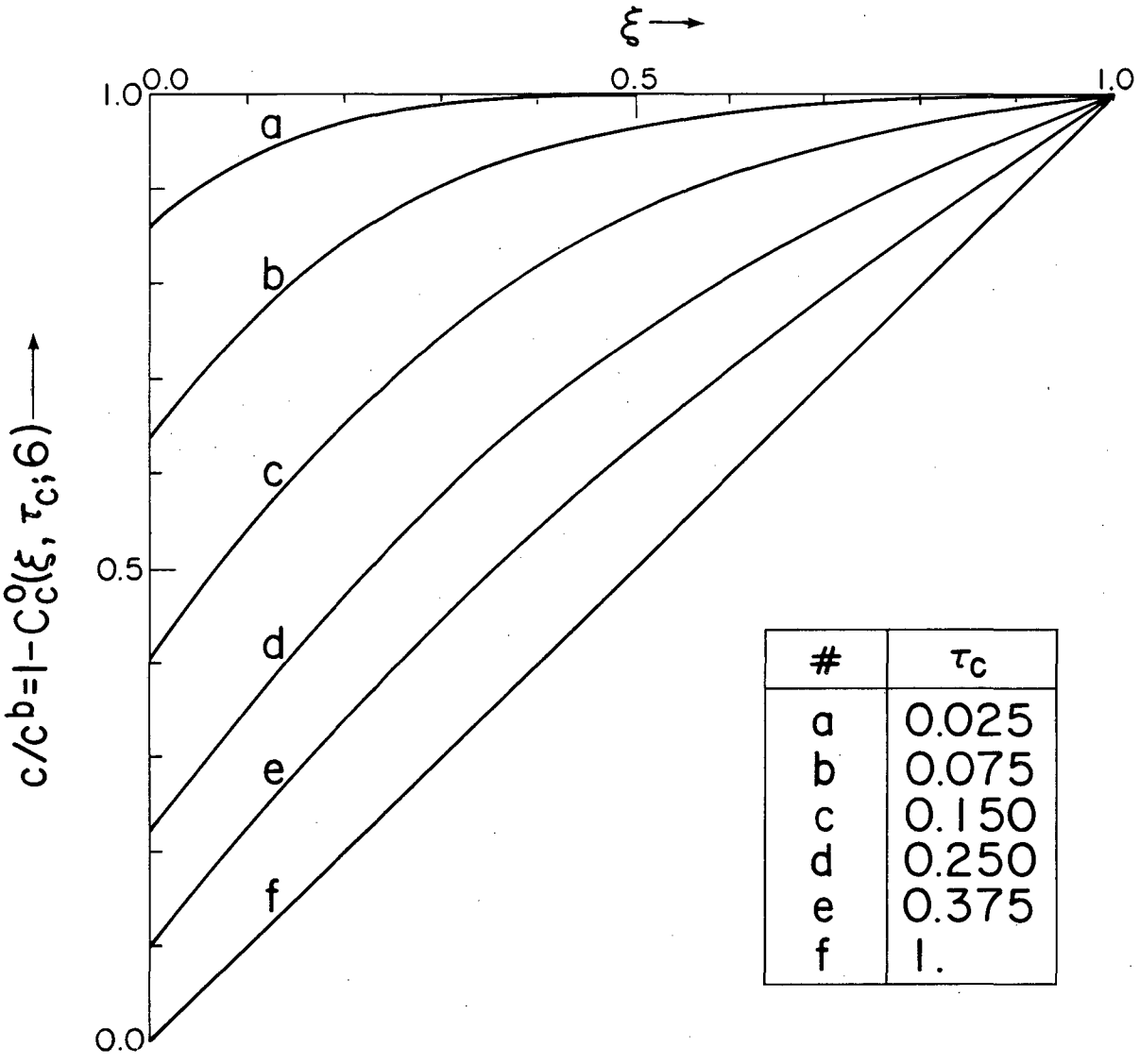
ξ →
0.0
0.5
1.0
1.0
0.5
0.0
c/c^b=1-C_c^0(ξ, τ_c;6) →
a
b
c
d
e
f
| τc
a | 0.025
b | 0.075
c | 0.150
d | 0.250
e | 0.375
f | 1.
XBL 825-618

Fig. 4b

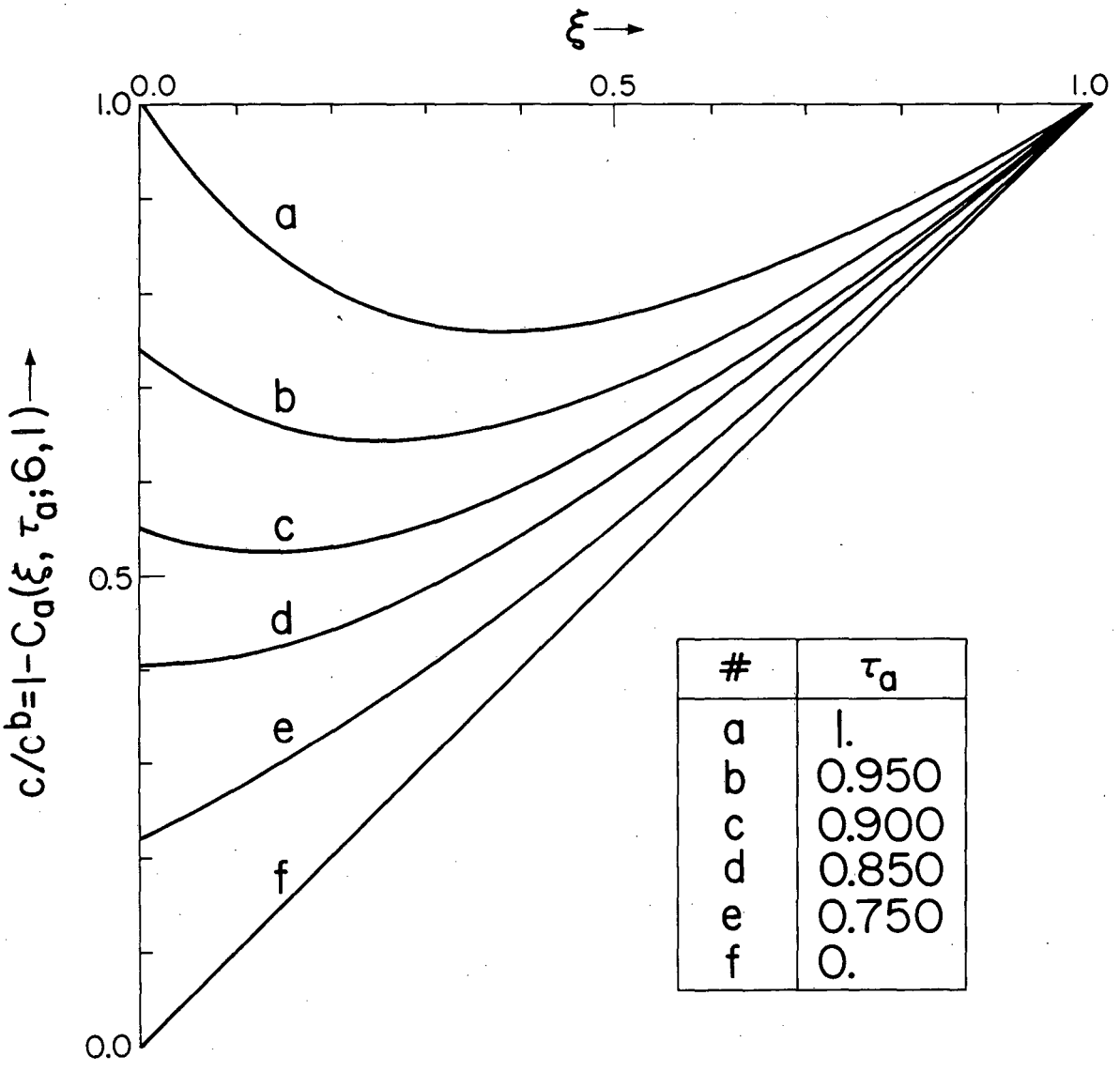
ξ →
0.0
0.5
1.0
1.0
0.5
0.0
c/c^b=1-C_a(ξ, τ_a;6,1) →
a
b
c
d
e
f
| τ_a
a | 1.
b | 0.950
c | 0.900
d | 0.850
e | 0.750
f | 0.
XBL 825-617

Fig. 4c

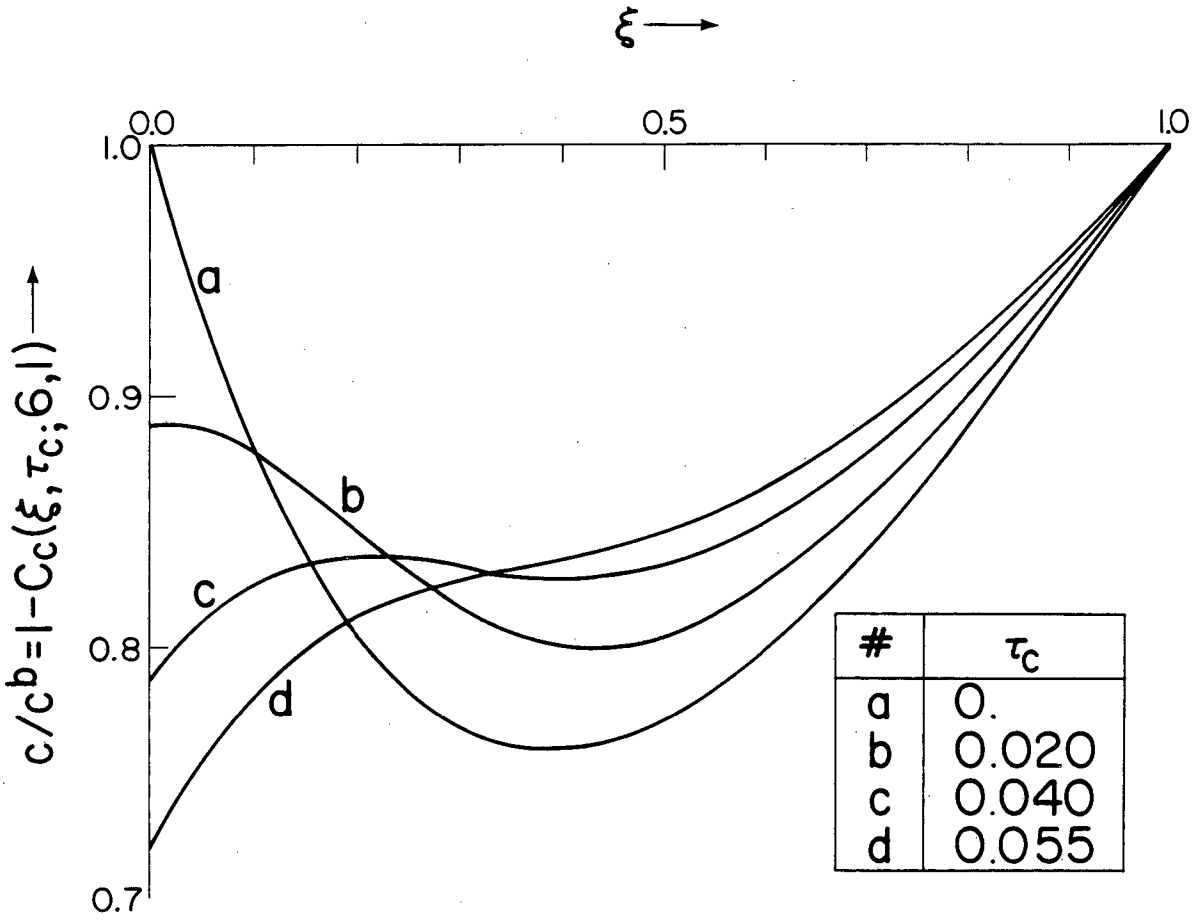

XBL 825-633

Fig. 4d

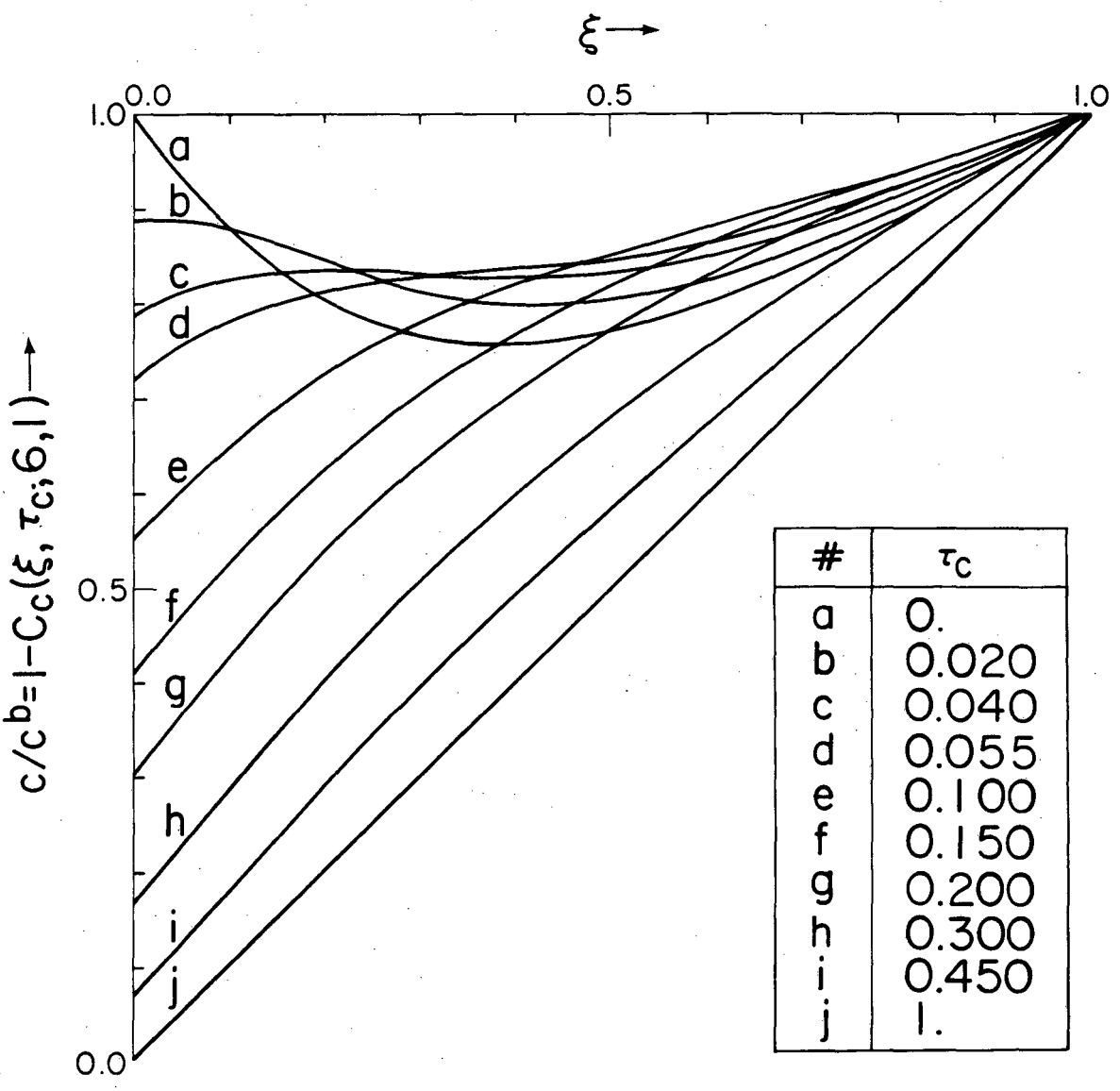

#	τ_c
a	0.
b	0.020
c	0.040
d	0.055
e	0.100
f	0.150
g	0.200
h	0.300
i	0.450
j	1.

XBL 825-621

Fig. 4e

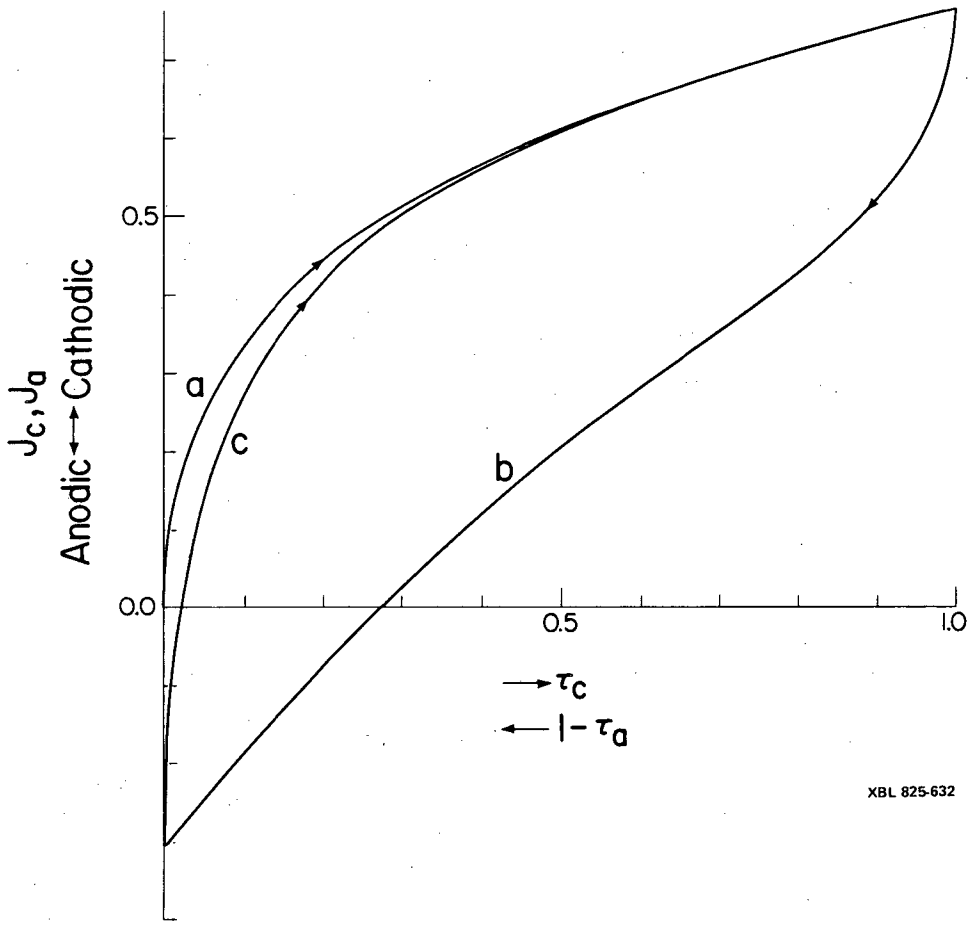
0.5
0.0
0.5
1.0
a
b
c
J_c, J_a
Anodic ← → Cathodic
$\rightarrow \tau_c$
$\leftarrow 1-\tau_a$
XBL 825-632

Fig. 5a

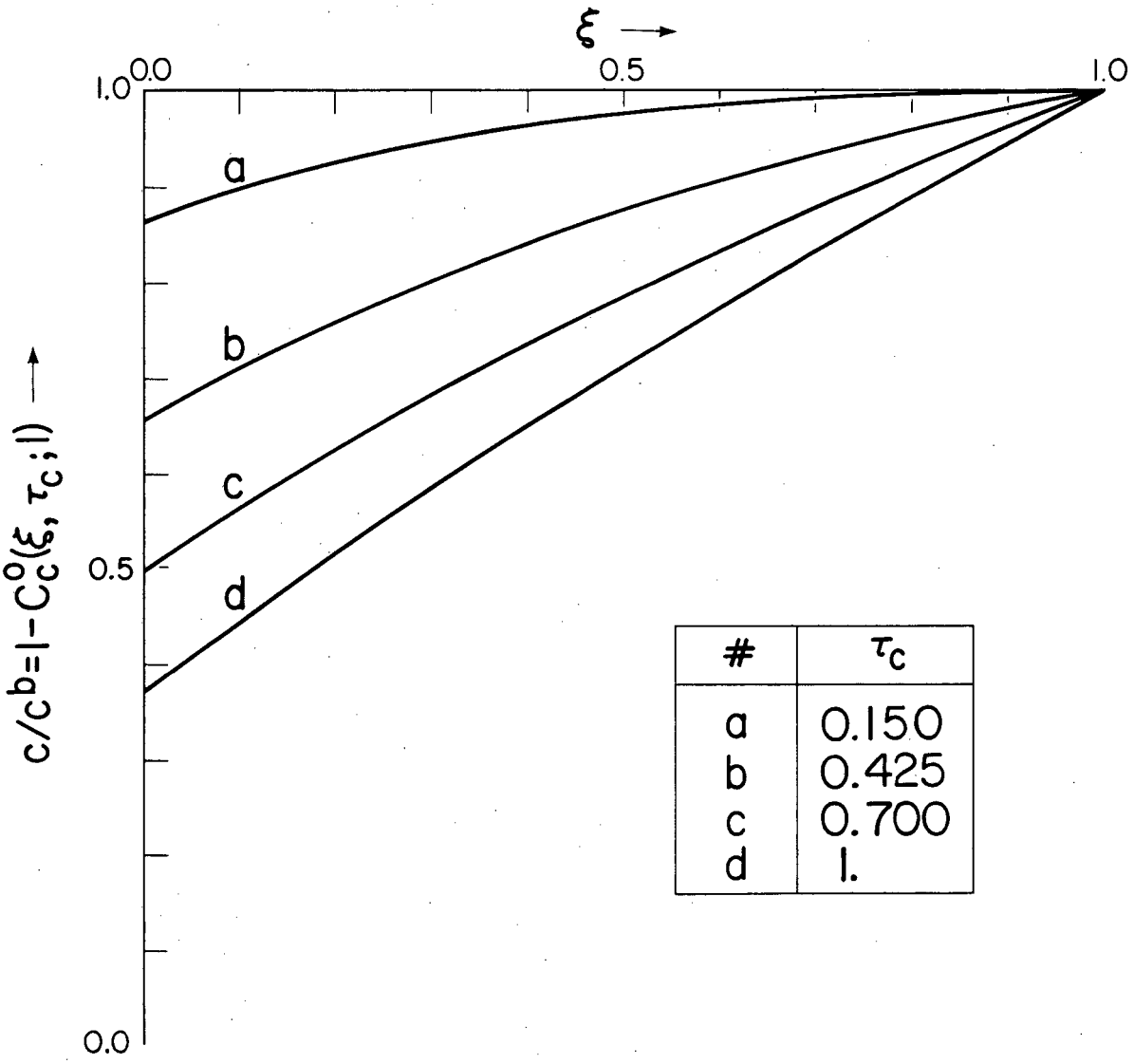

#	τ_c
a	0.150
b	0.425
c	0.700
d	1.

XBL 825-636

Fig. 5b

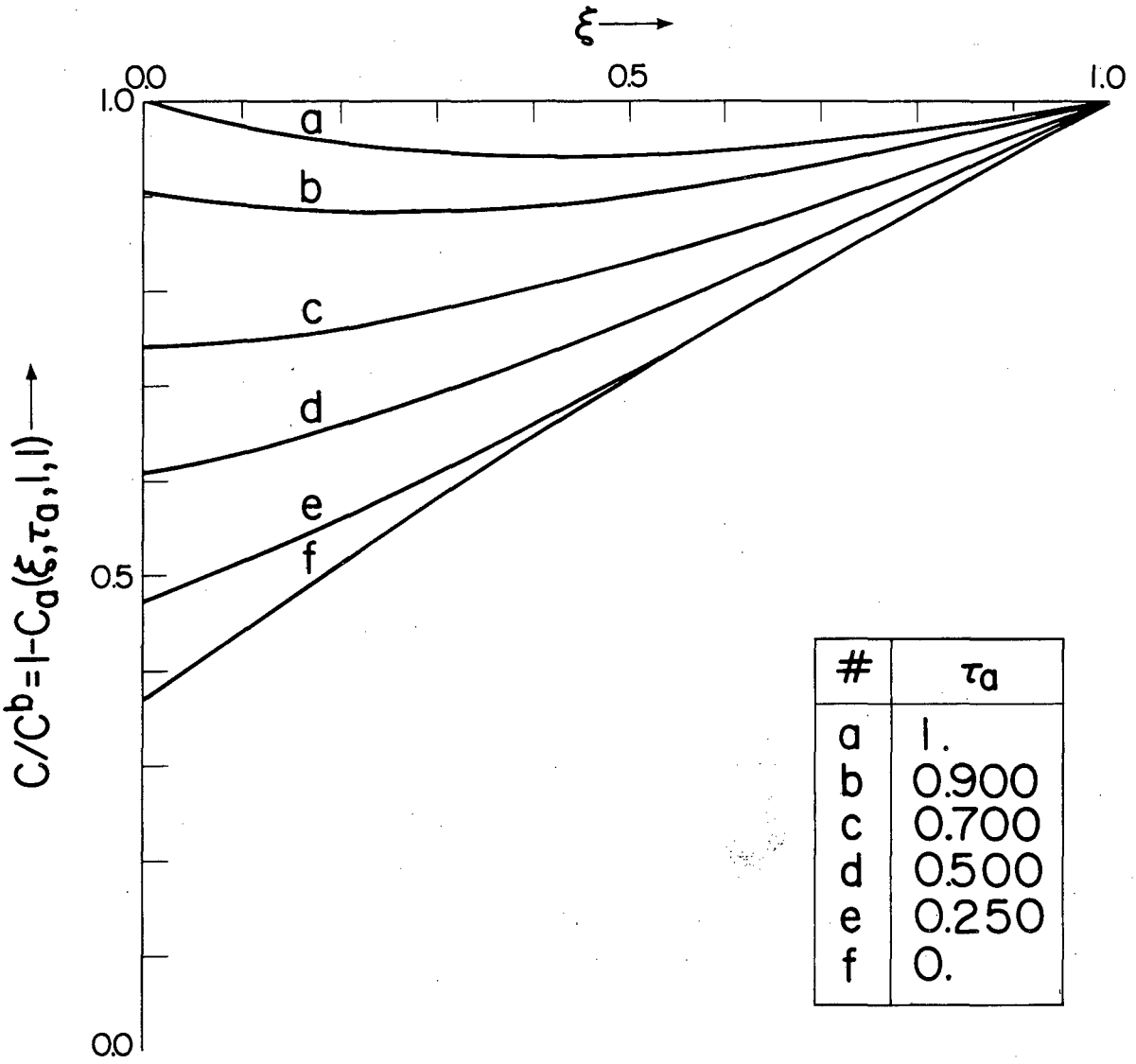
ξ⟶
0.0
0.5
1.0
1.0
0.5
0.0
C/C^b=1-C_a(ξ,τ_a,1,1)⟶
a
b
c
d
e
f
| τa
a | 1.
b | 0.900
c | 0.700
d | 0.500
e | 0.250
f | 0.
XBL 825-631

Fig. 5c

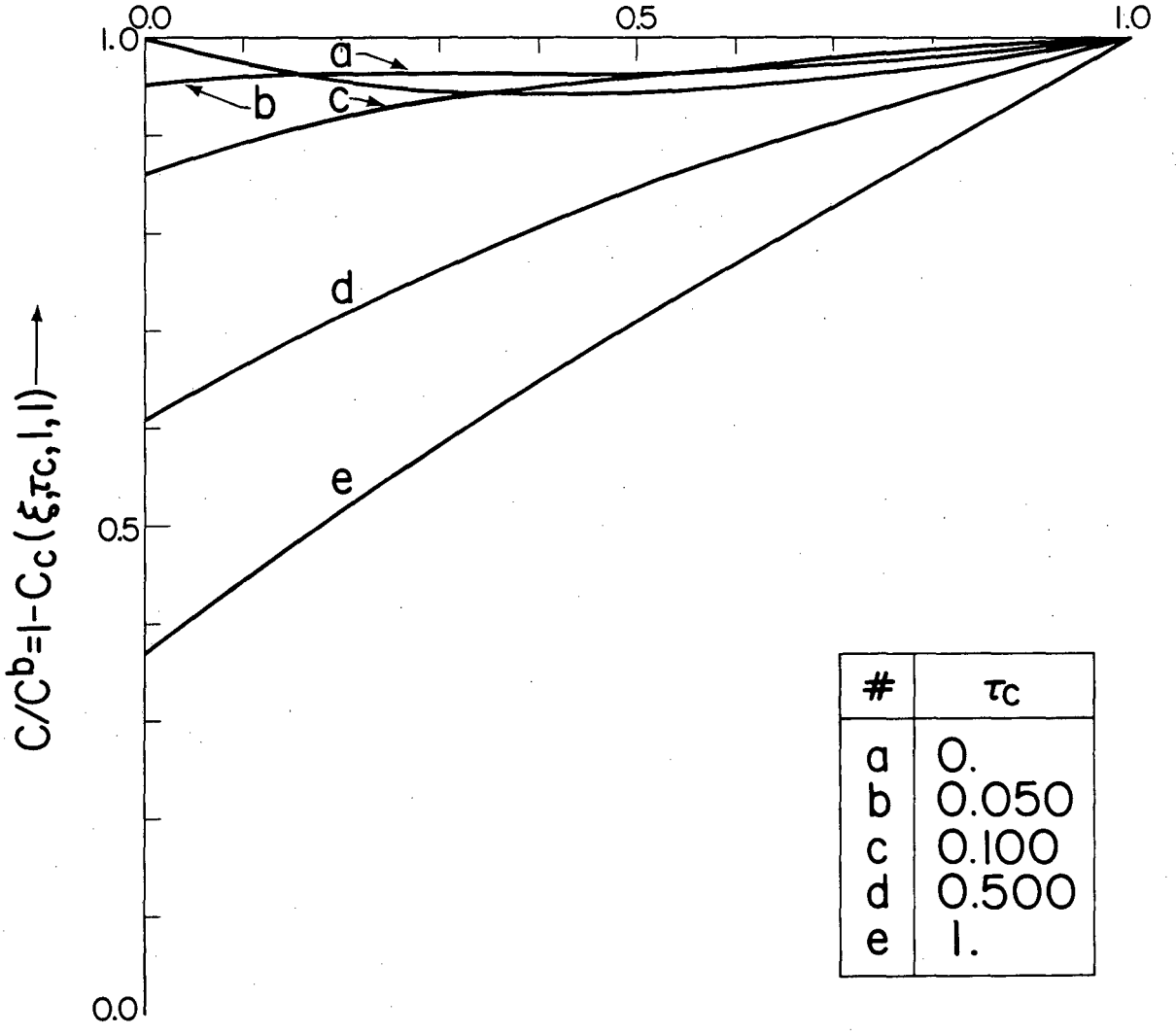

XBL 825-637

Fig. 5d

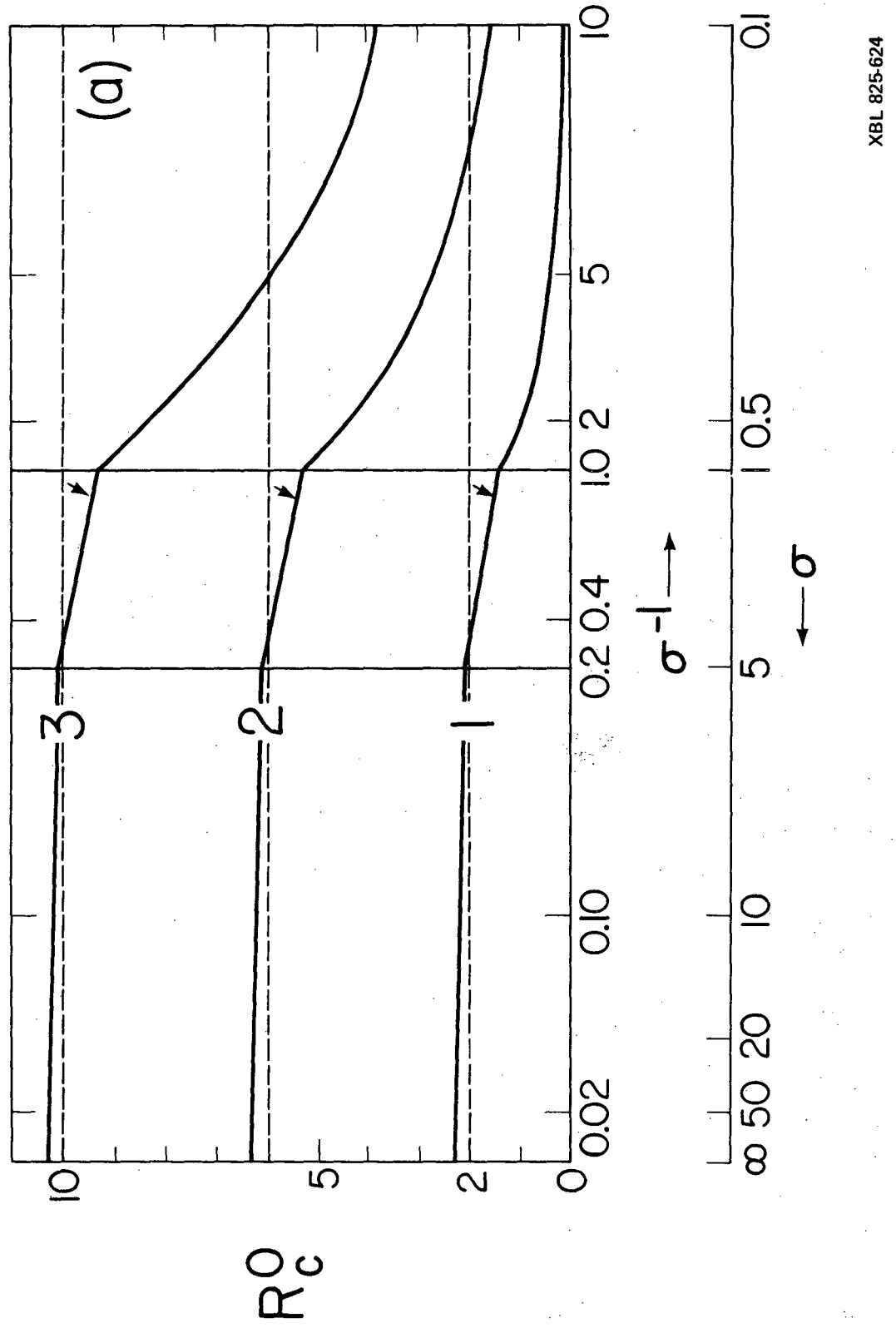

XBL 825-624

Fig. 6a

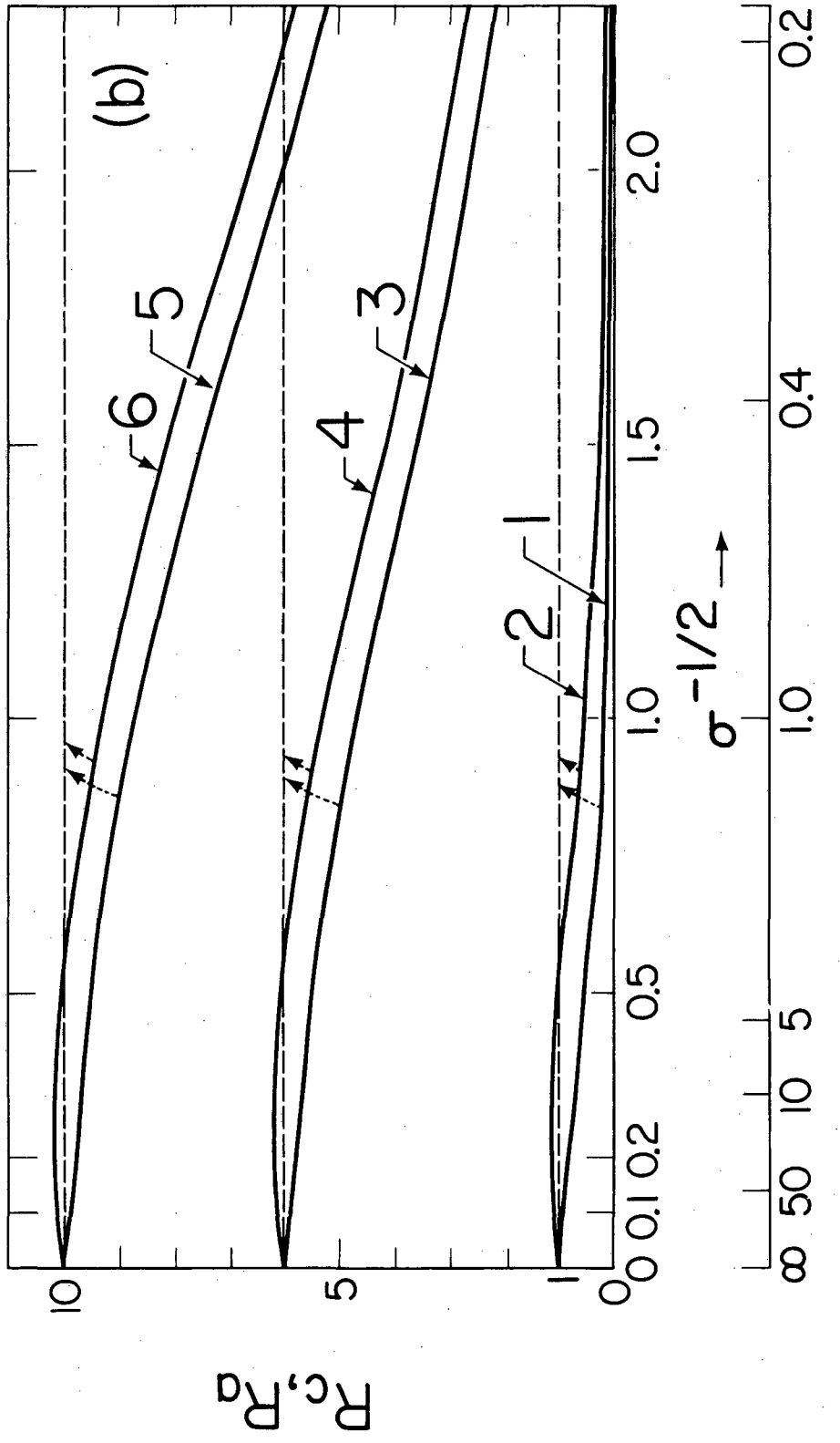

XBL 825-622

Fig. 6b

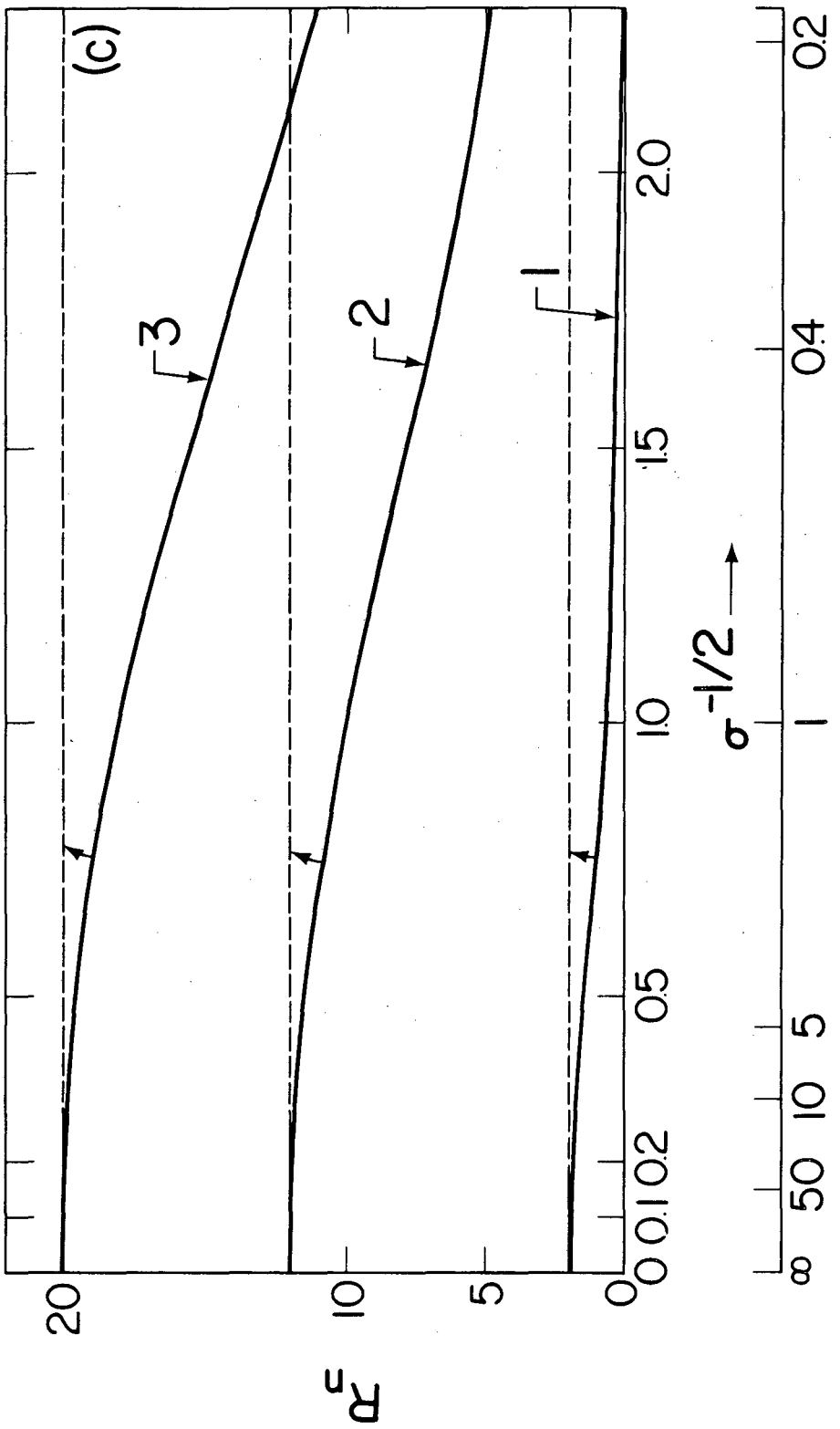

XBL 825-623

Fig. 6c

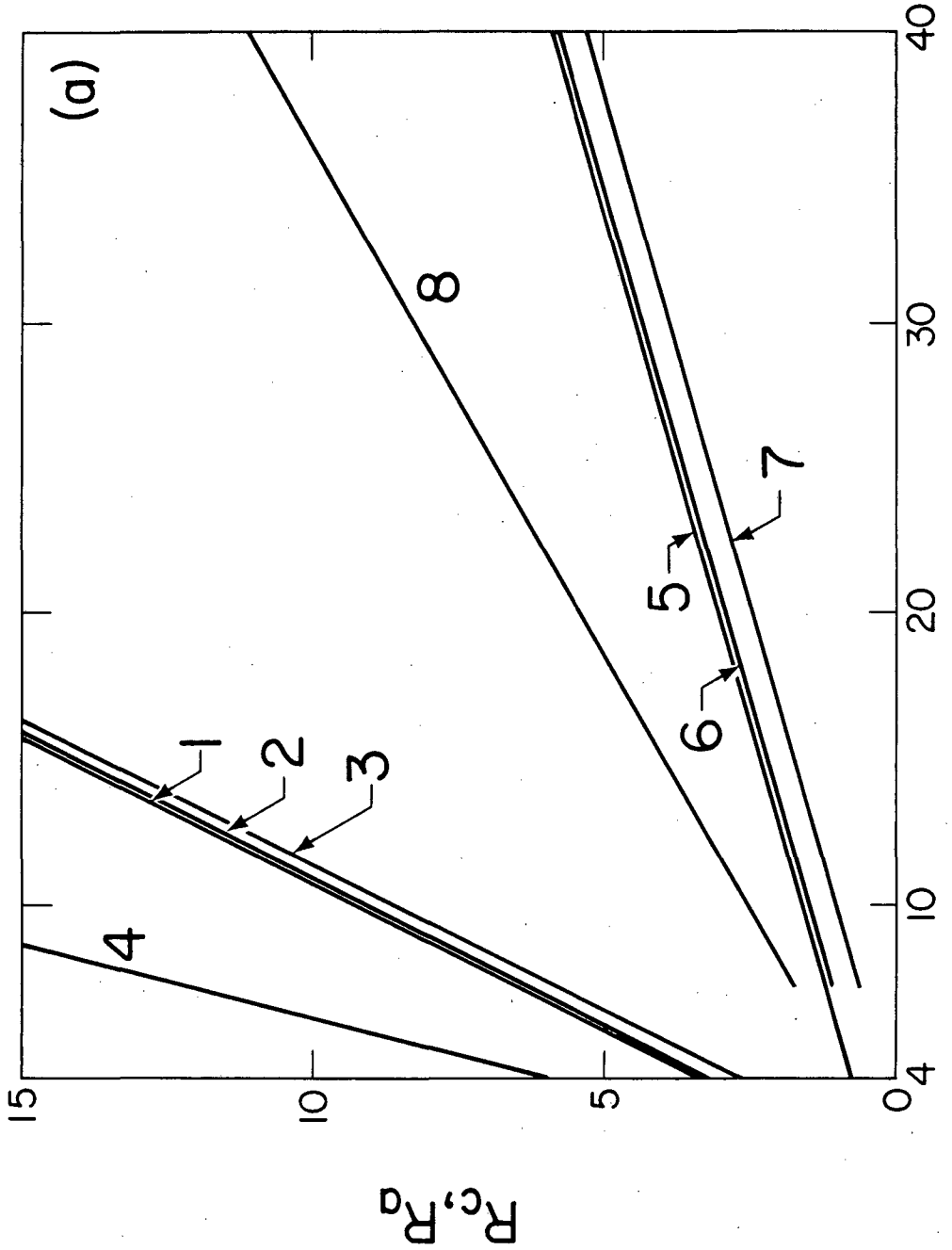

XBL 825-626

Fig. 7a

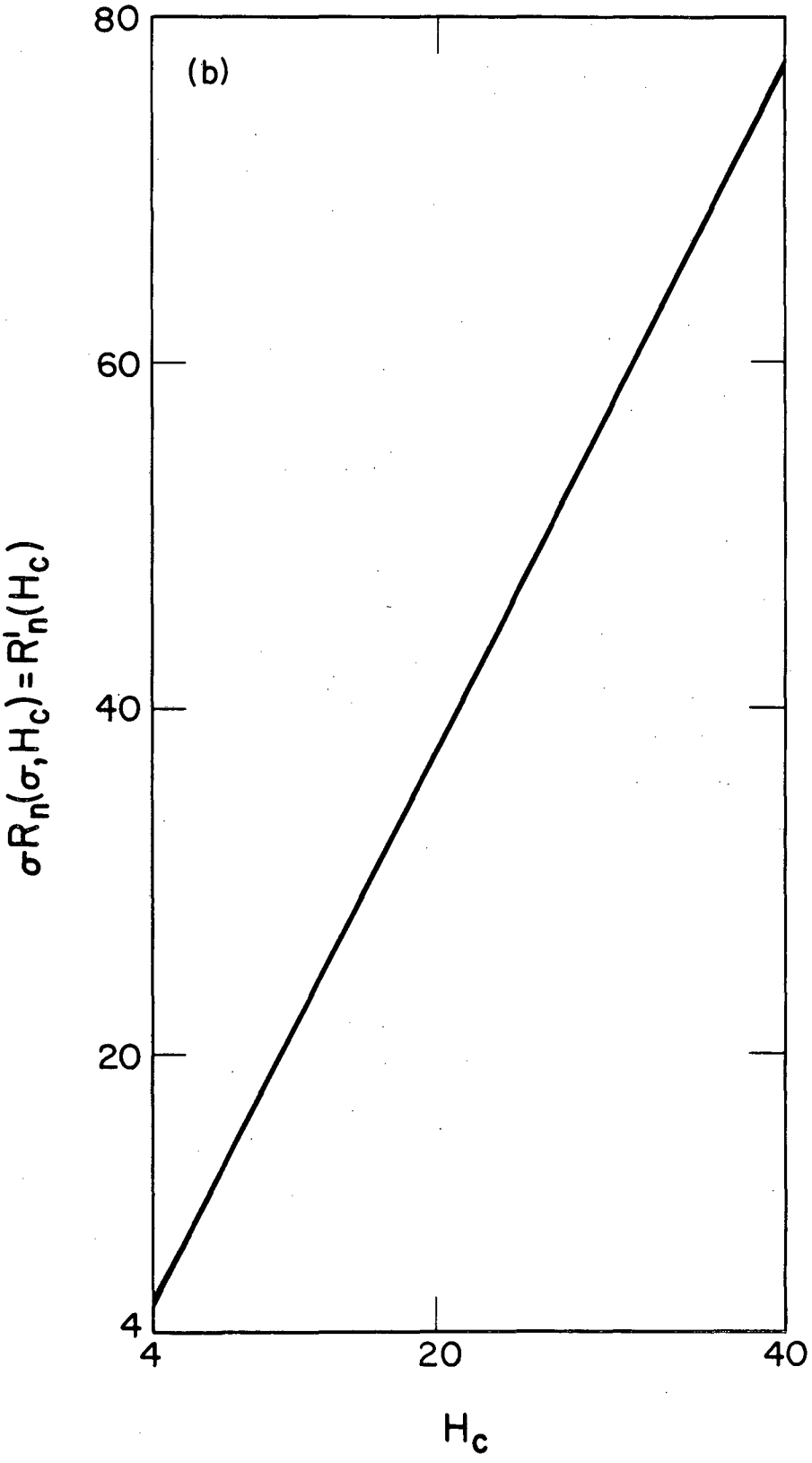

XBL 825-630

Fig. 7b

APPENDIX

Mathematical Derivation of Concentration, Current and Charge Density Functions

Letting δ be the thickness of the Levich diffusion layer, dimensionless quantities are introduced by eq. [A1]:

$$\xi = x/\delta \; ; \; \tau = Dt/\delta^2; \; C(\xi,\tau) = 1 - c/c^b \qquad [A1]$$

where D is the diffusion coefficient of the ion being deposited and ξ,τ,C are dimensionless distance, time, and concentration, respectively. Figure 1a shows the dependence of applied potential on dimensionless time. The initial value of the potential is E_{eq}, the electrode equilibrium potential computed from the Nernst equation on the basis of c^b. At a constant rate of v volts$\cdot$sec^{-1}, the potential is changed in the cathodic direction for θ sec until it reaches E_c, the cathodic reversal potential. θ' is a dimensionless reversal time,

$$\theta' = D\theta/\delta^2 \qquad [A2]$$

During the "anodic" cycle, the potential returns to its original value at the same rate. The first cathodic sweep refers to LSV, the first complete cycle is single sweep CV and several cycle to multi-sweep CV.

A combination of the RDE characteristic time, δ^2/D, characteristic voltage, RT/nF, and v yield a dimensionless sweep rate, σ:

$$\sigma = \frac{nF}{RT} \cdot v \cdot \frac{\delta^2}{D} \qquad [A3]$$

where n,F,R, and T have their usual meaning. As demonstrated in prior LSV-RDE theory (4-7), σ is a parameter of special significance. Since the initial potential has been assumed to be E_{eq}, the potential axis is also one of overpotential, beginning at 0 and ending at the cathodic reversal overpotential, η_c. Figure 1b shows the time

dependence of the surface concentration obtained from the Nernst equation:

$$C(0,\tau) = \begin{cases} 1 - \exp(2n\sigma\theta')\exp(-\sigma\tau) & ; \ 2n\theta' \leqslant \tau \leqslant (2n+1)\theta' \ ; \text{ cathodic cycle} \\ 1 - \exp[-(2n+2)\sigma\theta']\exp(\sigma\tau) & ; \ (2n+1)\theta' \leqslant \tau \leqslant (2n+2)\theta' ; \text{ anodic cycle} \end{cases} \quad [A4]$$

a. Concentration Functions

In order to derive expressions for $C(\xi,\tau)$ we introduce another function, $C_s(\xi,\tau)$, which is the solution to the problem when an infinite overpotential is applied to the RDE. Then,

$$C_s(0,\tau) = 1 \quad [A5]$$

i.e. the surface concentration drops to 0 at the instant the infinite potential step is applied. The reason shy $C_s(\xi,\tau)$ is introduced is that $C(\xi,\tau)$ can be obtained from $C_s(\xi,\tau)$ by an integral transform known as Duhamel's (or superposition) theorem (8,9). Since the initial conditions for the dimensionless functions are 0, it holds that

$$\overline{C}(\xi,p) = p.\ \overline{C}(0,p)\ .\ \overline{C}_s(\xi,p) \quad [A6]$$

where p is the Laplace parameter and $\overline{C}(0,p)$, $\overline{C}_s(\xi,p)$ are the Laplace transforms of $C(0,\tau)$ and $C_s(\xi,\tau)$, respectively; $\overline{C}(\xi,p)$ is the Laplace transform of $C(\xi,\tau)$, our unknown function. Equation [6] can be inverted by convolution in several ways. The most convenient turns our to result from associating p with $\overline{C}(0,p)$, to yield

$$C(\xi,\tau) = \int_0^\tau \frac{\partial C}{\partial \tau}(0,\lambda) \cdot C_s(\xi,\tau-\lambda)\, d\lambda \qquad [A7]$$

where λ is a dummy variable of integration. Note that

$$C_s(\xi,\tau) = 1-\xi + 2 \sum_{j=1}^{\infty} f_j(\xi) \cdot \exp(-j^2\pi^2\tau) \qquad [A8]$$

$$f_j(\xi) = (-1)^j (j\pi)^{-1} \sin[(1-\xi)j\pi] \qquad [A9]$$

While performing the integration indicated by eq. [A7], it is convenient to express time in terms of the number of cycles, and time into a cathodic or anodic sweep. We can thus write (fig. 1a):

$$\tau = 2\ell\theta' + \tau_c \quad ; 0 \leq \tau_c \leq \theta' \; ; \text{ cathodic sweep} \qquad [A10a]$$

$$\tau = (2\ell+1)\theta' + \tau_a \quad ; 0 \leq \tau_a \leq \theta' \; ; \text{ anodic sweep} \qquad [A10b]$$

where τ_c is dimensionless time into a cathodic sweep, τ_a is time into an anodic sweep, and ℓ is the number of complete cycles which have already been applied. The outcome of the integration in eq. [A7] are two concentration functions, one for the cathodic sweep and one for the anodic sweep. Apart from ξ and τ_c (or τ_a), these will depend on ℓ and on the two parameters, σ and θ'. We thus extend the symbol $C(\xi,\tau)$ to $C_c^\ell(\xi,\tau_c;\sigma,\theta')$ to describe the dimensionless concentration during the $(\ell+1)^{th}$ cathodic sweep (i.e. after the passage of ℓ complete cycles). The corresponding symbol for the concentration during the $(\ell+1)^{th}$ anodic sweep is $C_a^\ell(\xi,\tau_a;\sigma,\theta')$. For the special case of single sweep CV, $\ell=0$, the cathodic (also LSV) function is independent of θ'. The notation for this case

then is $C_c^{\,0}(\xi,\tau_c;\sigma)$ and $C_a^{\,0}(\xi,\tau_a;\sigma,\theta')$. The following results are obtained:

i) single sweep CV; cathodic (also LSV):

$$C_c^{\,0}(\xi,\tau_c;\sigma) = (1-\xi)[1-\exp(-\sigma\tau_c)] + 2\sigma\exp(-\sigma\tau_c)\sum_{J=1}^{\infty} f_j(\xi)(j^2\pi^2-\sigma)^{-1}$$
$$-2\sigma \sum_{j=1}^{\infty} f_j(\xi)\exp(-j^2\pi^2\tau_c)(j^2\pi^2-\sigma)^{-1} \qquad [A11]$$

ii) single sweep CV; anodic:

$$C_a^{\,0}(\xi,\tau_a;\sigma,\theta') = (1-\xi)[1-\exp(-\sigma\theta')\exp(\sigma\tau_a)] + 2\sigma\exp(-\sigma\theta')\sum_{j=1}^{\infty} f_j(\xi)(j^2\pi^2-\sigma)^{-1}$$
$$-2\sigma\sum_{j=1}^{\infty} f_j(\xi)\exp(-j^2\pi^2\tau_a)\exp(-j^2\pi^2\theta')(j^2\pi^2-\sigma)^{-1} - 2\sigma\exp(-\sigma\theta')$$
$$\exp(\sigma\tau_a)\sum_{j=1}^{\infty} f_j(\xi)(j^2\pi^2+\sigma)^{-1}$$
$$+2\sigma\exp(-\sigma\theta')\sum_{j=1}^{\infty} f_j(\xi)\exp(-j^2\pi^2\tau_a)(j^2\pi^2+\sigma)^{-1} \qquad [A12]$$

iii) multi-sweep CV; cathodic:

$$C_c^{\,\ell}(\xi,\tau_c;\sigma,\theta') = (1-\xi)[1-\exp(-\sigma\tau_c)] + 2\sigma\exp(-\sigma\tau_c)\sum_{j=1}^{\infty} f_j(\xi)(j^2\pi^2-\sigma)^{-1}$$
$$-2\sigma\sum_{j=1}^{\infty} f_j(\xi)\exp(-j^2\pi^2\tau_c)(j^2\pi^2-\sigma)^{-1}$$
$$-2\sigma\sum_{n=1}^{\ell}\sum_{j=1}^{\infty} f_j(\xi)\exp(-j^2\pi^2\tau_c)\exp(-2nj^2\pi^2\theta')(j^2\pi^2-\sigma)^{-1}$$
$$+2\sigma\exp(-\sigma\theta')\sum_{n=1}^{\ell}\sum_{j=1}^{\infty} f_j(\xi)\exp(-j^2\pi^2\tau_c)\exp[-(2n-1)j^2\pi^2\theta'](j^2\pi^2-\sigma)^{-1}$$
$$+2\sigma\exp(-\sigma\theta')\sum_{n=1}^{\ell}\sum_{j=1}^{\infty} f_j(\xi)\exp(-j^2\pi^2\tau_c)\exp[-(2n-1)j^2\pi^2\theta'](j^2\pi^2+\sigma)^{-1}$$
$$-2\sigma\sum_{n=1}^{\ell}\sum_{j=1}^{\infty} f_j(\xi)\exp(-j^2\pi^2\tau_c)\exp[-(2n-2)(j^2\pi^2+\sigma)^{-1} \qquad [A13]$$

iv) multi-sweep CV; anodic:

$$C_a^{\ell}(\xi,\tau_a;\sigma,\theta') = (1-\xi)[1-\exp(-\sigma\theta')\exp(\sigma\tau_a)] - 2\sigma\exp(-\sigma\theta')\exp(\sigma\tau_a)$$
$$\sum_{j=1}^{\infty} f_j(\xi)(j^2\pi^2+\sigma)^{-1} + 2\sigma\exp(-\sigma\theta')\sum_{j=1}^{\infty} f_j(\xi)\exp(-j^2\pi^2\tau_a)(j^2\pi^2+\sigma)^{-1}$$
$$- 2\sigma\sum_{n=0}^{\ell}\sum_{j=1}^{\infty} f_j(\xi)\exp(-j^2\pi^2\tau_a)\exp[-(2n+1)j^2\pi^2\theta'](j^2\pi^2-\sigma)^{-1}$$
$$+ 2\sigma\exp(-\sigma\theta')\sum_{n=0}^{\ell}\sum_{j=1}^{\infty} f_j(\xi)\exp(-j^2\pi^2\tau_a)\exp(-2nj^2\pi^2\theta')(j^2\pi^2-\sigma)^{-1}$$
$$+ 2\sigma\exp(-\sigma\theta')\sum_{n=1}^{\ell}\sum_{j=1}^{\infty} f_j(\xi)\exp(-j^2\pi^2\tau_a)\exp(-2nj^2\pi^2\theta')(j^2\pi^2+\sigma)^{-1}$$
$$- 2\sigma\sum_{n=1}^{\ell}\sum_{j=1}^{\infty} f_j(\xi)\exp(-j^2\pi^2\tau_a)\exp[-(2n-1)j^2\pi^2\theta'](j^2\pi^2+\sigma)^{-1} \qquad [A14]$$

Several terms in eqs. [A12]-[A14] contain the expression $\exp(-kj^2\pi^2\theta')$ where k usually is a non-zero integer. Even when k=1, the largest value that this term can take is $\exp(-j^2\pi^2\theta')$. For $\theta'\geq 1$, terms multiplied by $\exp(-kj^2\pi^2\theta')$ are very small and can be eliminated, rendering eqs.[A12]-[A14] much simpler; furthermore, both C_c^{ℓ} and C_a^{ℓ} become independent of ℓ. The physical interpretation of this is that the first anodic potential sweep and the second cathodic sweep yield concentrations which are periodic functions of time, irrespective of the value of σ, provided that $\theta'\geq 1$. The restriction on θ' is not limiting since when $\theta'=1$, the dimensional reversal time is of the order of δ^2/D, which is a small number. In the elimination of terms containing $\exp(-kj^2\pi^2\theta')$ care should be taken to retain terms for which k=0. The following results are obtained:

v) multi-sweep CV; periodic cathodic:

$$C_c(\xi,\tau_c;\sigma,\geq 1) = (1-\xi)[1-\exp(-\sigma\tau_c)] + 2\sigma\exp(-\sigma\tau_c)\sum_{j=1}^{\infty} f_j(\xi)(j^2\pi^2-\sigma)^{-1}$$
$$- 4\sigma\sum_{j=1}^{\infty} f_j(\xi)\, j^2\pi^2\exp(-j^2\pi^2\tau_c)(j^4\pi^4-\sigma^2)^{-1} \qquad [A15]$$

vi) multi-sweep CV; periodic anodic

$$C_a(\xi,\tau_a;\sigma,\geqslant 1) = (1-\xi)[1-\exp(-\sigma\theta')\exp(\sigma\tau_a)] - 2\sigma\exp(-\sigma\theta')\exp(\sigma\tau_a)$$
$$\sum_{j=1}^{\infty} f_j(\xi)(j^2\pi^2+\sigma)^{-1}$$
$$+ 4\sigma\exp(-\sigma\theta')\sum_{j=1}^{\infty} f_j(\xi)\, j^2\pi^2 \exp(-j^2\pi^2\tau_a)(j^4\pi^4-\sigma^2)^{-1} \qquad [A16]$$

One should note that the periodic concentration is independent of θ'. The notation chosen for the periodic functions does not include a dependence on ℓ; also, we use the symbol $\geqslant 1$ in place of θ', to emphasize the restriction on θ' for quick attainment of the periodic state.

b. Current Density Functions

We define the current density functions, J, as ratios of the current density to the diffusion limiting current density, i_L. J is dimensionless and, in general, will depend on τ_c (or τ_a), the number of cycles, ℓ, and the parameters σ and θ'. The notation for the current density function during a cathodic sweep is thus $J_c^{\ell}(\tau_c;\sigma,\theta')$, and $J_a^{\ell}(\tau_a;\sigma,\theta')$ for the subsequent anodic sweep. Expressions for J's can be derived either by application of Duhamel's transformation or by differentiation of the concentration functions at the surface. In essence, both methods are identical; however, if expressions for C's are not available, a suitable form of Duhamel's theorem yields J's directly. Since

$$\frac{i(\tau)}{i_L} = -\frac{\partial C}{\partial \xi}(0,\tau) \qquad [A17]$$

it follows from eq. [A7] that

$$\frac{i(\tau)}{i_L} = -\int_0^{\tau} \frac{\partial C}{\partial \tau}(0,\lambda)\cdot\frac{\partial C_s}{\partial \xi}(0,\tau-\lambda)\,d\lambda \qquad [A18]$$

$$\frac{\partial C}{\partial \xi}(0,\tau) = -\left[1 + 2\sum_{j=1}^{\infty} \exp(-j^2\pi^2\tau)\right] = -\theta_3(0,\pi i\tau) \qquad [A19]$$

θ_3 is one of the theta functions (11) whose relevance in RDE modeling under the Nernst-Siver approximation has been repeatedly demonstrated (4-6). We can then write

$$\frac{i(\tau)}{i_L} = \int_0^{\tau} \frac{\partial C}{\partial \tau}(0,\lambda) \cdot \theta_3(0,\pi i(\tau-\lambda))\, d\lambda \qquad [A20]$$

and compute J_c^{ℓ} and J_a^{ℓ} using eq. [A10]. Alternatively,

$$J_c^{\ell}(\tau_c;\, \sigma,\theta') = -\frac{\partial C_c}{\partial \xi}(0,\tau_c;\, \sigma,\theta') \qquad [A21a]$$

$$J_a^{\ell}(\tau_a;\, \sigma,\theta') = -\frac{\partial C_a^{\ell}}{\partial \xi}(0,\tau_a;\, \sigma,\theta') \qquad [A21b]$$

where eqs. [A13] and [A14] can be used for the differentiations. Once expressions for J_c^{ℓ} and J_a^{ℓ} are available, the same elimination of terms containing $\exp(-kj^2\pi^2\theta')$, $k \geq 1$, can be done as previously, for $\theta' \geq 1$. Physically, this means that after the first cathodic (LSV) sweep, the current during the first anodic, second cathodic and so on is in the periodic state, i.e. does not change with further cycling. It turns out that when the value of the dimensionless sweep rate σ exceeds ca. 3, J_c^{ℓ} exhibits a maximum both during the first and periodic sweeps; after the maximum, its value decreases to i_L. When $\sigma \lesssim 3$, J_c^{ℓ} increases to i_L monotonically. In terms of dimensional time, attainment of i_L experimentally during the LSV sweep would guarantee that subsequent currents are periodic. However, this is not necessary since the criterion for periodicity is $\theta' \geq 1$,

irrespective of whether i_L is reached within δ^2/D or not.

It should be noted here that when $\theta'<1$, a periodic behavior of J_c^{ℓ} and J_a^{ℓ} is expected to be reached as $\ell\to\infty$; furthermore, the two periodic states may in general be different; i.e. $J_c(\tau_c;\ \sigma,\geq 1) \neq J_c^{\infty}(\tau_c;\ \sigma,<1)$ and $J_a(\tau_a;\ \sigma,\geq 1) \neq J_a^{\infty}(\tau_a;\ \sigma,<1)$. The detailed behavior of J_c^{∞} and J_a^{∞} has not been investigated, since reversal times significantly less than δ^2/D are not expected to be of experimental importance. Expressions for the current density functions are as follows:

i) single-sweep CV; cathodic (LSV)(4):

$$J_c^{0}(\tau_c;\sigma) = 1 - \sigma^{1/2}\cot(\sigma^{1/2})\exp(-\sigma\tau_c) - 2\sigma\sum_{j=1}^{\infty}\exp(-j^2\pi^2\tau_c)(j^2\pi^2-\sigma)^{-1} \qquad [A22]$$

ii) single-sweep CV; anodic:

$$J_a^{0}(\tau_a;\ \sigma,\theta') = 1-\sigma^{1/2}\coth(\sigma^{1/2})\exp(-\sigma\theta')\exp(\sigma\tau_a)-2\sigma\sum_{j=1}^{\infty}\exp(-j^2\pi^2\theta')\exp(-j^2\pi^2\tau_a)(j^2\pi^2-\sigma)^{-1} + 4\sigma\exp(-\sigma\theta')\sum_{j=1}^{\infty} j^2\pi^2\exp(-j^2\pi^2\tau_a)(j^4\pi^4-\sigma^2)^{-1} \qquad [A23]$$

iii) multi-sweep CV; cathodic:

$$J_c^{\ell}(\tau_c;\ \sigma,\theta') = 1- \sigma^{1/2}\cot(\sigma^{1/2})\exp(-\sigma\tau) - 2\sigma\sum_{j=1}^{\infty}\exp(-j^2\pi^2\tau_c)(j^2\pi^2-\sigma)^{-1} - 2\sigma\sum_{n=1}^{\ell}\sum_{j=1}^{\infty}\exp(-j^2\pi^2\tau_c)\exp(-2n\ j^2\pi^2\theta')(j^2\pi^2-\sigma)^{-1} + 2\sigma\exp(-\sigma\theta')\sum_{n=1}^{\ell}\sum_{j=1}^{\infty}\exp(-j^2\pi^2\tau_c)\exp[-(2n-1)j^2\pi^2\theta'](j^2\pi^2-\sigma)^{-1} + 2\sigma\exp(-\sigma\theta')\sum_{n=1}^{\ell}\sum_{j=1}^{\infty}\exp(-j^2\pi^2\tau_c)\exp[-(2n-1)j^2\pi^2\theta'](j^2\pi^2+\sigma)^{-1}$$

$$- 2\sigma \sum_{n=1}^{\ell} \sum_{j=1}^{\infty} \exp(-j^2\pi^2\tau_c) \exp[-(2n-2)j^2\pi^2\theta'](j^2\pi^2+\sigma)^{-1} \qquad [A24]$$

iv) multi-sweep CV; anodic:

$$J_a^{\ell}(\tau_a;\ \sigma,\theta') = 1-\sigma^{1/2}\coth(\sigma^{1/2}) \exp(-\sigma\theta')\exp(\sigma\tau_a) + 2\sigma \exp(-\sigma\theta') \sum_{j=1}^{\infty}$$

$$\exp(-j^2\pi^2\tau_a)(j^2\pi^2+\sigma)^{-1}$$

$$- 2\sigma \sum_{n=0}^{\ell} \sum_{j=1}^{\infty} \exp(-j^2\pi^2\tau_a) \exp[-(2n+1)\ j^2\pi^2\theta'](j^2\pi^2-\sigma)^{-1}$$

$$+ 2\sigma\exp(-\sigma\theta') \sum_{n=1}^{\ell} \sum_{j=1}^{\infty} \exp(-j^2\pi^2\tau_a) \exp(-2nj^2\pi^2\theta')(j^2\pi^2+\sigma)^{-1}$$

$$+ 2\sigma\exp(-\sigma\theta') \sum_{n=0}^{\ell} \sum_{j=1}^{\infty} \exp(-j^2\pi^2\tau_a) \exp(-2nj^2\pi^2\theta')(j^2\pi^2-\sigma)^{-1}$$

$$-2\sigma \sum_{n=1}^{\ell} \sum_{j=1}^{\infty} \exp(-j^2\pi^2\tau_a) \exp[-(2n-1)j^2\pi^2\theta'](j^2\pi^2+\sigma)^{-1} \qquad [A25]$$

v) multi-sweep CV; periodic cathodic:

$$J_c(\tau_c;\ \sigma,\geqslant 1) = 1-\sigma^{1/2}\cot(\sigma^{1/2})\exp(-\sigma\tau_c) - 4\sigma \sum_{j=1}^{\infty} j^2\pi^2\exp(-j^2\pi^2\tau_c)$$

$$(j^4\pi^4-\sigma^2)^{-1} \qquad [A26]$$

vi) multi-sweep CV; periodic anodic:

$$J_a(\tau_a;\ \sigma,\geqslant 1) = 1- \sigma^{1/2}\coth(\sigma^{1/2})\exp(-\sigma\theta')\exp(\sigma\tau_a) + 4\sigma \exp(-\sigma\theta')$$

$$\sum_{j=1}^{\infty} j^2\pi^2 \exp(-j^2\pi^2\tau_a)(j^4\pi^4-\sigma^2)^{-1} \qquad [A27]^{\dagger}$$

---

†The identities $\sum_{j=1}^{\infty} 2\sigma(j^2\pi^2-\sigma)^{-1} = 1-\sigma^{1/2}\cot(\sigma^{1/2})$ and $\sum_{j=1}^{\infty} 2\sigma(j^2\pi^2+\sigma)^{-1}$ $= \sigma^{1/2}\coth(\sigma^{1/2})-1$ have been used in the derivations (12).

c. Charge Density Functions

We define charge density functions, R, as ratios of the charge density to a characteristic charge density. The latter quantity is the product of a characteristic current density, i_L, with a characteristic time, δ^2/D, and represents the charge per unit electrode area that would be deposited over a time δ^2/D were the current constant and equal to i_L. We choose R on a per cycle basis instead of a cumulative quantity which would describe deposit accumulation during a complete multi-sweep experiment. There are three types of such functions: R_c^{ℓ} is the charge function associated with the $(\ell+1)^{th}$ cathodic sweep; R_a^{ℓ} is associated with the $(\ell+1)^{th}$ anodic sweep; and R_n^{ℓ} is the net charge deposited during the complete $(\ell+1)^{th}$ cycle; obviously,

$$R_n^{\ell} = R_c^{\ell} + R_a^{\ell} \qquad [A28]$$

From their definition,

$$R_c^{\ell}(\sigma,\theta') = \int_0^{\theta'} J_c^{\ell}(\tau_c;\ \sigma,\theta')d\tau_c;\ R_a^{\ell}(\sigma,\theta') = \int_0^{\theta'} J_a^{\ell}(\tau_a;\ \sigma,\theta')d\tau_a \qquad [A29]$$

note that R's are only functions of σ and θ' since they are integrals of J's over τ. By performing the integrations indicated in eq.[A29], the following expressions are obtained:

i) multi-sweep CV; cathodic:

$$R_c^{\ell}(\sigma,\theta') = \theta' - \sigma^{-1/2}\cot(\sigma^{1/2})[1-\exp(-\sigma\theta')] - 2\sigma \sum_{j=1}^{\infty} [1-\exp(-j^2\pi^2\theta')]$$
$$[j^2\pi^2(j^2\pi^2-\sigma)]^{-1}$$

$$- 2\sigma \sum_{n=1}^{\ell} \sum_{j=1}^{\infty} \exp[-(2n-2)j^2\pi^2\theta'][j^2\pi^2(j^2\pi^2+\sigma)]^{-1}$$

$$+ \sum_{n=1}^{\ell} \sum_{j=1}^{\infty} \exp[-(2n-1)j^2\pi^2\theta'][4\sigma\, j^2\pi^2\exp(-\sigma\theta') + 2\, j^2\pi^2-2\sigma^2]$$

$$[j^2\pi^2(j^4\pi^4-\sigma^2)]^{-1}$$

$$- \sum_{n=1}^{\ell} \sum_{j=1}^{\infty} \exp(-2nj^2\pi^2\theta')[4\sigma\, j^2\pi^2\exp(-\sigma\theta') + 2\sigma j^2\pi^2 + 2\sigma^2]$$

$$[j^2\pi^2(j^4\pi^4-\sigma^2]^{-1}$$

$$+ 2\sigma \sum_{n=1}^{\ell} \sum_{j=1}^{\infty} \exp[-(2n+1)j^2\pi^2\theta'][j^2\pi^2(j^2\pi^2-\sigma)]^{-1} \qquad [A30]$$

ii) multi-sweep CV; anodic:

$$R_a^{\ell}(\sigma,\theta') = \theta' - \sigma^{-1/2}\coth(\sigma^{1/2})[1-\exp(-\sigma\theta')] + 2\sigma \exp(-\sigma\theta') \sum_{j=1}^{\infty}$$

$$[1-\exp(-j^2\pi^2\theta')][j^2\pi^2(j^2\pi^2+\sigma)]^{-1}$$

$$+ 2\sigma \exp(-\sigma\theta') \sum_{j=1}^{\infty} [1-\exp(-j^2\pi^2\theta')][j^2\pi^2(j^2\pi^2-\sigma)]^{-1}$$

$$- 2\sigma \sum_{j=1}^{\infty} \exp(-j^2\pi^2\theta')\, [j^2\pi^2(j^2\pi^2-\sigma)]^{-1}$$

$$- 2\sigma \sum_{n=1}^{\ell} \sum_{j=1}^{\infty} \exp[-(2n-1)j^2\pi^2\theta'][j^2\pi^2(j^2\pi^2+\sigma)]^{-1}$$

$$+ \sum_{n=1}^{\ell} \sum_{j=1}^{\infty} \exp(-2nj^2\pi^2\theta')[4\sigma\, j^2\pi^2\exp(-\sigma\theta') + 2\sigma\, j^2\pi^2-2\sigma^2]$$

$$[j^2\pi^2(j^4\pi^4-\sigma^2)]^{-1}$$

$$- \sum_{n=1}^{\ell} \sum_{j=1}^{\infty} \exp[-(2n+1)j^2\pi^2\theta'][4\sigma\, j^2\pi^2\exp(-\sigma\theta') + 2\sigma\, j^2\pi^2+2\sigma^2]$$

$$[j^2\pi^2(j^4\pi^4-\sigma^2)]^{-1}$$

$$+ 2\sigma \sum_{n=0}^{\ell} \sum_{j=1}^{\infty} \exp(-(2n+2)j^2\pi^2\theta'][j^2\pi^2(j^2\pi^2-\sigma]^{-1} \qquad [A31]$$

Simplifications of eqs. [A30] and [A31] yields expressions for $R_c(\sigma,\geqslant 1)$ and $R_a(\sigma,\geqslant 1)$. The following are equations for the charge density function during the LSV sweep, $R_c^{\,0}(\sigma,\theta')$, and the periodic cathodic, anodic, and net charge density functions, $R_c(\sigma,\geqslant 1)$, $R_a(\sigma,\geqslant 1)$, and $R_n(\sigma,\geqslant 1)$, respectively.

$$R_c^{\,0}(\sigma,\theta') = \theta' + 1/3 - \sigma^{-1} + \sigma^{-1/2}\cot(\sigma^{1/2})\exp(-\sigma\theta') \qquad [A32]$$

$$R_c(\sigma,\geqslant 1) = \theta' - 2\sigma^{-1} + \sigma^{-1/2}\cot(\sigma^{1/2})\exp(-\sigma\theta') + \sigma^{-1/2}\coth(\sigma^{1/2}) \qquad [A33]$$

$$R_a(\sigma,\geqslant 1) = \theta' + 2\sigma^{-1}\exp(-\sigma\theta') - \sigma^{-1/2}\cot(\sigma^{1/2})\exp(-\sigma\theta') - \sigma^{-1/2}\coth(\sigma^{1/2}) \qquad [A34]$$

$$R_n(\sigma,\geqslant 1) = 2\theta' - 2\sigma^{-1}\,[1-\exp(-\sigma\theta')] \qquad [A35]$$

Often repeated application of de ℓ' Hôpital's rule yields

$$\lim_{\sigma\to 0} R = 0 \qquad [A36]$$

which is in agreement with intuitive expectation but is not obvious in eqs. [A32-A35]. For large values of σ,

$$R_c^{\,0} \sim \theta' + 1/3 - \sigma^{-1} \text{ (linear dependence on } \sigma^{-1}) \; ; \; \sigma>>1 \qquad [A37]$$

$$\lim_{\sigma\to\infty} R_c^{\,0} = \theta' + 1/3 \qquad [A38]$$

The periodic cathodic function exhibits a maximum at $\sigma = 16$;

$$R_{c,max} = R_c(16,\geqslant 1) = \theta' + 1/8 \qquad [A39]$$

$$R_c \sim \theta' + \sigma^{-1/2} \text{ (linear dependence on } \sigma^{-1/2}) \; ; \; \sigma>>1 \qquad [A40]$$

$$\lim_{\sigma\to\infty} R_c = \theta' \qquad [A41]$$

Also,

$$\lim_{\sigma\to\infty} R_n = 2\theta' \qquad [A42]$$

$$R_n > 0,\ \sigma \neq 0 \qquad [A43]$$

Numerical investigation of charge densities indicates that they increase (except for R_c when $\sigma \geq 16$) with increasing σ, for a fixed value of θ'. However, this is the case when θ' is fixed. In usual experimental arrangements, the fixed parameter is the reversal overpotential, η_c. Expressing η_c as multiples of RT/nF, we introduce a dimensionless cathodic overpotential, H_c,

$$H_c = \eta_c/(RT/nF) = \sigma\theta' \qquad [A44]$$

The charge density functions can then be expressed in terms of σ and H_c as follows ($\theta' \geq 1$):

$$R_c^0(\sigma,H_c) = 1/3 + \sigma^{-1}(H_c-1) + \sigma^{-1/2}\cot(\sigma^{1/2})\exp(-H_c) \qquad [A45]$$

$$R_c(\sigma,H_c) = \sigma^{-1}(H_c-2) + \sigma^{-1/2}\cot(\sigma^{1/2})\exp(-H_c) + \sigma^{-1/2}\coth(\sigma^{1/2}) \qquad [A46]$$

$$R_a(\sigma,H_c) = \sigma^{-1}[H_c + 2\exp(-H_c)] - \sigma^{-1/2}\cot(\sigma^{1/2})\exp(-H_c) - \sigma^{-1/2}\coth(\sigma^{1/2}) \qquad [A47]$$

$$R_n(\sigma,H_c) = 2\sigma^{-1}[H_c + \exp(-H_c) - 1] \qquad [A48]$$

It should be noted that

$$\sigma R_n(\sigma,H_c) = R'_n(H_c) = 2[H_c + \exp(-H_c)-1] \qquad [A49]$$

i.e. R' is independent of σ and depends only on H_c. Obviously, for a fixed H_c, all charge density functions decrease with increasing σ. This point is better illustrated in the discussion of the equations thus far derived on their relevence to electroanalytical investigations.

Applicability of RDE Models Other Than the Nernst-Siver Approximation

Equation [A18] can be rewritten as follows:

$$\frac{i(\tau)}{i_L} = \int_0^\tau \frac{\partial C}{\partial \tau}(o,\lambda) \cdot \frac{i_s}{i_L}(o,\tau-\lambda)d\lambda \qquad [A50]$$

where i_s/i_L is the current density measured when a potential step is applied to a RDE such that the surface concentration is o for all $\tau \geq o$. As already mentioned,

$$\frac{i_s}{i_L}(\tau) = \theta_3(o,\pi i\tau) \qquad [A19]$$

when the Nernst-Siver approximation is used. Alternative expressions have been derived by Nisancloglu and Newman (8) and Viswanathan and Cheh (13). These are:
(Nisancioglu and Newman)

$$\frac{i_s(\tau)}{i_L} = 1 + \varepsilon \sum_{j=o}^{\infty} B_j \exp(-\varepsilon^2 \lambda_j \tau) \; ; \; \varepsilon = \Gamma(4/3)^* \qquad [A51]$$

---

*The factor $\Gamma(4/3)$ arises because Nisancioglu and Newman use different dimensionless parameters; e.g. $\zeta = \Gamma(4/3)\xi$, where ζ is dimensionless distance according to these authors and ξ is defined in eq. [A1].

(Viswanathan and Cheh)

$$\frac{i_{s(\tau)}}{i_L} = 1 + \sum_{j_1=1}^{\infty} C_{j_1} \exp(-\lambda^2_{j1}\tau) \qquad [A52]$$

Coefficients B_j, C_{j_1} and eigenvalues λ_j, λ_{j_1} have been computed numerically and reported in tabular form. Equations [A51] and [A52] are very similar. Equation [A52] was independently proposed specifically to treat diffusion problems related to pulsed potentials. Equations [A51] and [A52] predict identical results (to 4 significant figures) over their range of applicability. Combination of eq. [A50] with each of eq. [A51] and eq. [A52] yields expressions for the ℓ-dependent current density functions. For the $(\ell+1)$th cathodic sweep, these are as follows:

(Nisancioglu and Newman)

$$J_c^{\ell}(\tau_c;\sigma,\theta') = 1-\exp(-\sigma\tau_c) + \sigma\varepsilon \exp(-\sigma\tau_c) \sum_{j=o}^{\infty} B_j(\varepsilon^2\lambda_j-\sigma)^{-1}$$

$$-\sigma\varepsilon \sum_{j=o}^{\infty} B_j \exp(-\varepsilon^2\lambda_j\tau_c)(\varepsilon^2\lambda_j-\sigma)^{-1}$$

$$-\sigma\varepsilon \sum_{n=1}^{\ell} \sum_{j=o}^{\infty} B_j \exp[-(2n-2)\varepsilon^2\lambda_j\theta'] \exp(-\varepsilon^2\lambda_j\tau_c)(\varepsilon^2\lambda_j+\sigma)^{-1}$$

$$+\sigma\varepsilon \exp(-\sigma\theta') \sum_{n=1}^{\ell} \sum_{j=o}^{\infty} B_j \exp[-(2n-1)\varepsilon^2\lambda_j\theta']\exp(-\varepsilon^2\lambda_j\tau_c)(\varepsilon^2\lambda_j-\sigma)^{-1}$$

$$+\sigma\varepsilon \exp(-\sigma\theta') \sum_{n=1}^{\ell} \sum_{j=o}^{\infty} B_j \exp[-(2n-1)\varepsilon^2\lambda_j\theta']\exp(-\varepsilon^2\lambda_j\tau_c)(\varepsilon^2\lambda_j+\sigma)^{-1}$$

$$-\sigma\varepsilon \sum_{n=1}^{\ell} \sum_{j=o}^{\infty} B_j \exp(-2n\varepsilon^2\lambda_j\theta') \exp(-\varepsilon^2\lambda_j\tau_c)(\varepsilon^2\lambda_j-\sigma)^{-1} \qquad [A53]$$

(Viswanathan and Cheh)

$$J_c^{\ell}(\tau_c;\sigma,\theta') = 1-\exp(-\sigma\tau_c) + \sigma \exp(-\sigma\tau_c) \sum_{j_1=1}^{\infty} C_{j_1}(\lambda_{j_1}^2-\sigma)^{-1}$$

$$- \sigma \sum_{j_1=1}^{\infty} C_{j_1} \exp(-\lambda_{j_1}^2\tau_c)(\lambda_{j_1}^2-\sigma)^{-1}$$

$$- \sigma \sum_{n=1}^{\ell} \sum_{j_1=1}^{\infty} C_{j_1} \exp[-(2n-2)\lambda_{j_1}^2\theta']\exp(-\lambda_{j_1}^2\tau_c)(\lambda_{j_1}^2+\sigma)^{-1}$$

$$+ \sigma\exp(-\sigma\theta') \sum_{n=1}^{\ell} \sum_{j_1=1}^{\infty} C_{j_1} \exp[-(2n-1)\lambda_{j_1}^2\theta']\exp(-\lambda_{j_1}^2\tau_c)(\lambda_{j_1}^2-\sigma)^{-1}$$

$$+ \sigma\exp(-\sigma\theta') \sum_{n=1}^{\ell} \sum_{j_1=1}^{\infty} C_{j_1} \exp[-(2n-1)\lambda_{j_1}^2\theta']\exp(-\lambda_{j_1}^2\tau_c)(\lambda_{j_1}^2+\sigma)^{-1}$$

$$- \sigma \sum_{n=1}^{\ell} \sum_{j_1=1}^{\infty} C_{j_1} \exp(-2n\lambda_{j_1}^2\theta')\exp(-\lambda_{j_1}^2\tau_c)(\lambda_{j_1}^2-\sigma)^{-1} \qquad [A54]$$

Equations [A53] and [A54] could in principle be used to yield values for J_c^{ℓ}. However, the number of published coefficients and eigenvalues is not sufficient to guarantee convergence of the series to the desired accuracy, even at large τ_c, due to the presence of terms such as $\Sigma\ B_j(\varepsilon^2\lambda_j-\sigma)^{-1}$ and $\Sigma\ C_{j_1}(\lambda_{j_1}^2-\sigma)^{-1}$. This constitutes an additional reason for applying the Nernst-Siver approximation.

TECHNICAL INFORMATION DEPARTMENT
LAWRENCE BERKELEY LABORATORY
UNIVERSITY OF CALIFORNIA
BERKELEY, CALIFORNIA 94720